5
Beam Bending and Column Buckling

Although we have not emphasized it, we now note some standard terminology. Generally, a structural member having one dimension much greater than the other two is called a *rod* if it is subjected to a tensile axial load, it is called a *column* if it is subjected to a compressive axial load, it is called a *shaft* if it is circular in cross section and subjected to a torque, and it is called a *beam* if it is subjected to moments or transverse loads that induce bending.[1] In this chapter, we focus on beams as well as columns that buckle (i.e., structural members having one dimension much greater than the other two and that bend laterally when loaded). As in Chap. 4, we limit our examination to structural members that exhibit a linearly elastic, homogeneous, and isotropic (LEHI) behavior over small strains. Hence, again, the primary biomedical applications are (long) bones as well as select biomaterials. In addition, just as in Chap. 4, we will see that the topics herein are essential to the design of many different load cells, which, in turn, are important to many different areas of biomedical engineering, from gait analysis to studying mechanotransduction in cells. As in prior chapters, however, the most important thing is the deepening of one's understanding of the general approach of mechanics, not the specific (textbook) applications or solutions.

Whereas most engineering students learn about "bending moment and shear force diagrams" in a first course on engineering, here we briefly review these ideas because of their importance and because of the nonunique sign conventions and approaches used in different textbooks. In other words, we need to be

[1] For completeness, note that structural members having two dimensions much greater than the third are called plates or shells if they are initially flat or curved, respectively. An example of the latter is the skull. If a plate or shell does not resist bending, it is called a membrane. The pericardium is an example of a curved membrane.

J.D. Humphrey, S.L. O'Rourke, *An Introduction to Biomechanics*,
DOI 10.1007/978-1-4939-2623-7_5

on the same page when we begin our analysis of stress and deformation in subsequent sections.

5.1 Shear Forces and Bending Moments

Given a generic straight beam (Fig. 5.1), we extract a differential element of length Δx and note the exposed shear forces V and bending moments M_z (i.e., bending moments about the z axis). We recall from statics that V and M_z can vary with position x; hence, the values on the left exposed face need not equal the values on the right face. Question: By how much do they differ? Because the right face is a distance Δx from the left, we expect that moments and shears on the right to differ from those on the left by only some small amount, say $M_z + \Delta M_z$ and $V + \Delta V$ on the right x face relative to M_z and V on the left face. Recall, too, that if a body is in equilibrium, then each of its parts is in equilibrium. Hence, assuming the possible existence of a uniformly distributed load $q(x)$, let us enforce equilibrium for the differential element in Fig. 5.1b. Force balance requires

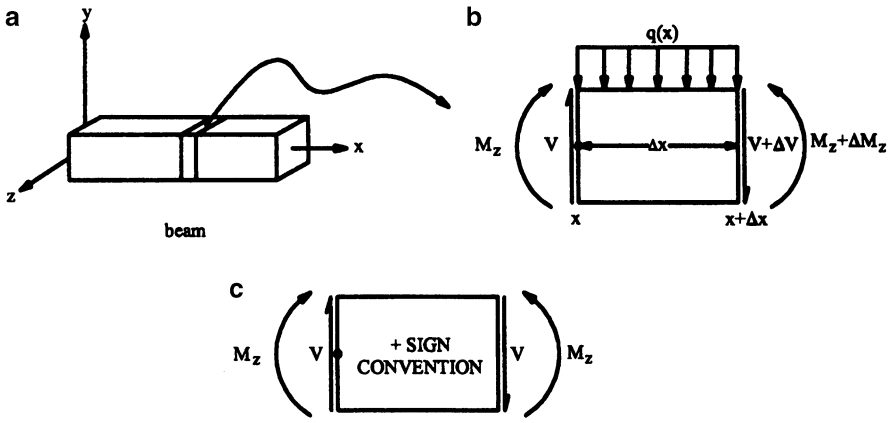

FIGURE 5.1 Panel **a** shows a generic initially straight beam and convenient coordinate system, with a representative section of length Δx isolated for removal via fictitious cuts. Panel **b** shows the removed differential element with an applied distributed load $q(x)$ and isolated internal shear forces V and bending moments M_z, each of which may vary as a function of location x. Panel **c** shows the positive sign convention that is adopted herein. Note: Although it is useful to consult other books for additional illustrative examples or alternate explanations and derivations, the sign convention differs considerably from book to book, which changes the governing equations and values of the computed quantities of interest. Paying careful attention to sign conventions is thus very important.

$$\sum F_x = 0 \rightarrow 0 = 0, \tag{5.1}$$

$$\sum F_y = 0 \rightarrow V - (V + \Delta V) - q(x)\Delta x = 0, \tag{5.2}$$

or

$$\Delta V = -q(x)\Delta x \rightarrow \frac{\Delta V}{\Delta x} = -q(x). \tag{5.3}$$

If we take the limit as Δx approaches zero, we obtain the general differential equation

$$\lim_{\Delta x \to 0} \frac{\Delta V}{\Delta x} = \frac{dV}{dx} \rightarrow \frac{dV}{dx} = -q(x). \tag{5.4}$$

Note that in this derivation, we assumed that the resultant of $q(x)$, $\left[\text{i.}e., \quad \int_x^{x+\Delta x} q(x)dx\right]$ is well approximated by $q(x)\Delta x$ over a small length Δx, which is to say that although q may vary with x, it will not vary much over the length Δx and, thus, it can be taken out of the integral. In other words, we invoke the mean value theorem for integrals from calculus.

Finally, let us enforce moment balance for the differential element in Fig. 5.1b (let point A exist at $x = 0$):

$$\sum M_z\big)_A = 0 \rightarrow -M_z + (M_z + \Delta M_z) - q(x)\Delta x\left(\frac{\Delta x}{2}\right) - (V + \Delta V)(\Delta x) = 0, \tag{5.5}$$

which reduces to

$$\Delta M_z = V\Delta x + \Delta V \Delta x + \frac{1}{2}q(x)(\Delta x)^2, \tag{5.6}$$

or

$$\frac{\Delta M_z}{\Delta x} = V + \Delta V + \frac{1}{2}q(x)\Delta x. \tag{5.7}$$

Finally, in the limit as we shrink Δx to a point (whereby ΔV and Δx go to zero), we have

$$\lim_{\Delta x \to 0} \frac{\Delta M_z}{\Delta x} = \lim_{\Delta x \to 0} \left[V + \Delta V + \frac{1}{2} q(x) \Delta x \right] = V \tag{5.8}$$

or our final result

$$\frac{dM_z}{dx} = V(x). \tag{5.9}$$

Equations (5.4) and (5.9) will prove very useful when we seek to draw the shear and bending moment diagrams. Next, let us consider a full analysis of a general beam problem.

When all of the forces are applied in one plane, we see that only three of the six equations of statics are available for the analysis. These are $\Sigma F_x = 0$, $\Sigma F_y = 0$, and $\Sigma M_z = 0$. In addition to providing our general differential equations, these equations also allow us to determine reaction forces at the supports of the beam. Indeed, the analysis of any beam or frame (i.e., finding internal forces and moments) should begin with a free-body diagram of the whole structure that shows both the applied and the reactive loads, which must satisfy equilibrium. The reactions can be computed using the equations of equilibrium provided that the system is statically determinate; in the case of statically indeterminate problems, which we consider below, additional equations are needed. Here, however, let us focus on the former, simpler case.

The next step in a general analysis uses the concept that if a body is in equilibrium, then each of its parts is also in equilibrium. We thus repeat the free-body diagram/equilibrium procedure for each judicious cut of interest. Consider an imaginary cut normal to the axis of the beam that separates the beam into two segments. Each of these segments is also in equilibrium. The conditions of equilibrium require the existence of internal forces and moments at each cut section of the beam. In general, at a section of such a member, at location x, a shear force $V(x)$, a horizontal force $f(x)$, and a moment $M_z(x)$ are necessary to maintain the isolated part in equilibrium. To illustrate this, consider initially straight, constant-cross-section LEHI beams in the following examples.

Example 5.1 For the beam in Fig. 5.2, find $V(x)$ and $M_z(x)$ and draw the resulting shear force and bending moment diagrams. P, a, b, and L are assumed to be known.

Solution: The first step in solving this problem is to draw a free-body diagram of the whole beam and then to determine the reaction forces at the supports using the equations of (statics) equilibrium; that is,

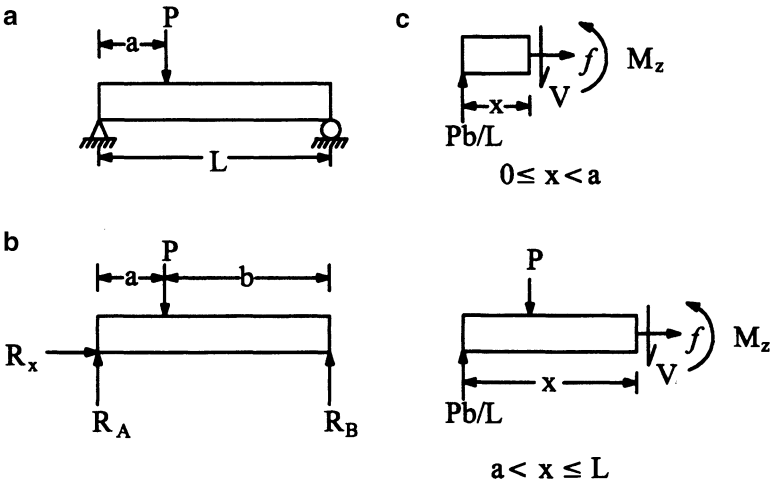

FIGURE 5.2 Shown here is a transversely loaded, simply supported beam (panel **a**), the free body of the whole structure (panel **b**), and free-body diagrams of two parts of the structure (panel **c**) that isolate the internal loads and moments in two regions of interest. Note: Remember that judicious cuts are often best taken between abrupt changes in loads, as done here.

$$\sum F_x = 0 \rightarrow R_x = 0,$$
$$\sum F_y = 0 \rightarrow R_A + R_B - P = 0,$$
$$\sum M_z)_A = 0 \rightarrow R_B L - Pa = 0,$$

where, from moment balance, we have

$$R_B = \frac{Pa}{L},$$

and with $L - a = b$, we now have, from vertical force balance,

$$R_A = P - \frac{Pa}{L} = P\left(1 - \frac{a}{L}\right) = P\left(\frac{L-a}{L}\right) = \frac{Pb}{L}.$$

The next step is to construct a free-body diagram for each part of interest, with judicious choices of cuts. In general, *we make cuts between any abrupt changes in load, geometry, or material properties* (see Fig. 5.2c). First, for the section cut to the left of the applied load P (i.e., for $0 < x < a$),

$$\sum F_x = 0 \rightarrow f = 0,$$
$$\sum F_y = 0 \rightarrow \frac{Pb}{L} - V = 0 \rightarrow V = \frac{Pb}{L},$$
$$\sum M_z)_A = 0 \rightarrow M_z - Vx = 0 \rightarrow M_z(x) = \left(\frac{Pb}{L}\right)x.$$

Similarly, for the section cut to the right of the applied load P (i.e., for $a < x < L$),

$$\sum F_x = 0 \rightarrow f = 0,$$
$$\sum F_y = 0 \rightarrow \frac{Pb}{L} - P - V = 0,$$

or

$$V = \frac{Pb}{L} - P = P\left(\frac{b}{L} - 1\right) = P\left(\frac{b-L}{L}\right) \rightarrow V = \frac{-Pa}{L},$$

and, finally,

$$\sum M_z)_A = 0 \rightarrow M_z - Pa - Vx = 0,$$
$$M_z = Pa - \frac{Pa}{L}x \rightarrow M_z(x) = Pa\left(1 - \frac{x}{L}\right).$$

Now that we have the functions $V(x)$ and $M_z(x)$ for each section of interest, we can construct the shear force and bending moment diagrams, recalling that

$$V(x) = \begin{cases} \dfrac{Pb}{L} & \text{for } x \in (0,a) \\ -\dfrac{Pa}{L} & \text{for } x \in (a,L) \end{cases} \quad \text{and} \quad M_z(x) = \begin{cases} \dfrac{Pb}{L}x & \text{for } x \in (0,a) \\ Pa\left(1 - \dfrac{x}{L}\right) & \text{for } x \in (a,L). \end{cases}$$

It is convenient to construct our shear and bending moment diagrams directly below the free-body diagram of the beam, using the same horizontal scale for the length of the beam (Fig. 5.3). Note, in particular, that the internal shear force is constant within each of the two sections of interest. Consistent with Eq. (5.9), the associated moments are each linear in these sections of interest, the slope of

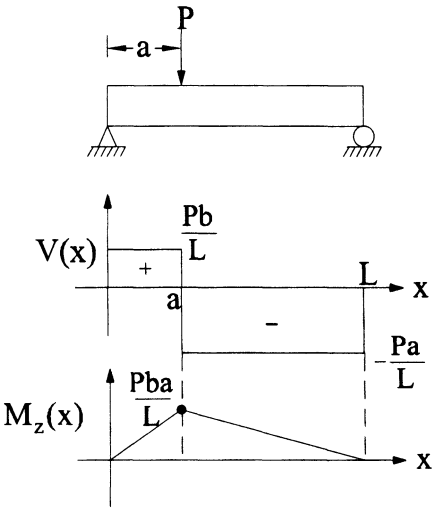

FIGURE 5.3 Shear and bending moment diagrams for the beam in Fig. 5.2. It is best to draw such diagrams as done here: Show the physical problem with the shear and bending diagrams directly below. This will help you to develop some intuition with regard to how such diagrams should look for various physical problems.

which is given by the value of V. Finally, note that there is a discontinuity (jump) in $V(x)$ where the transverse load P is applied, but there is no jump in $M_z(x)$ given the absence of any applied (concentrated) moment.

Example 5.2 The beam in Fig. 5.4 has a uniformly, or evenly, distributed load $q(x) = q_o$. Find V and M_z at all x and the resulting shear force and bending moment diagrams.

Solution: Again, the first step is to draw a free-body diagram of the whole structure and to determine the reaction forces at the supports using the equations of statics; that is,

$$\sum F_x = 0 \rightarrow R_x = 0,$$
$$\sum F_y = 0 \rightarrow R_y - \int_0^L q_o dx = 0 \quad \text{or} \quad R_y = q_o L.$$

Finally,

$$\sum M_z)_A = 0 \rightarrow -M_A - \int_0^L q_o x dx = 0 \quad \text{or} \quad M_A = -\frac{q_o L^2}{2}.$$

Before proceeding to equilibrium of parts, let us note the following. In your first course on statics, you may have solved this problem by considering force and

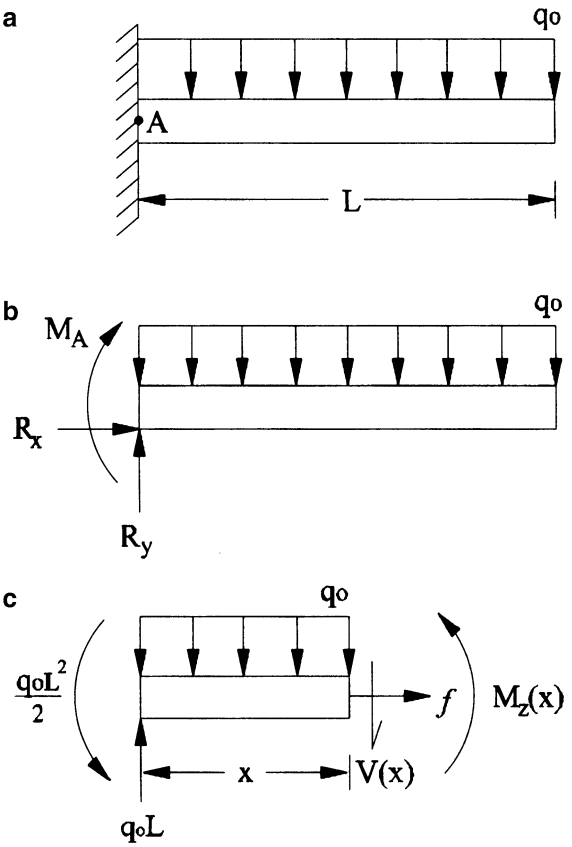

FIGURE 5.4 Shown is a uniformly loaded [i.e., $q(x) = q_o$] cantilevered beam (panel **a**) as well as free-body diagrams of the whole (panel **b**) and one part of the beam (panel **c**). Note that only one fictitious cut is needed to expose the internal loads and moments because there are no abrupt changes in geometry, properties, or loading between $x = 0$ and $x = L$.

moment balance in terms of the *resultant* force and moment due to the uniformly applied load $q(x) = q_o$. These resultants are

$$R_F = q_o L, \quad M_F = -q_o L\left(\frac{L}{2}\right).$$

which are seen easily. The reactions can thus be solved in terms of these resultants via equilibrium. Whereas this procedure is simple in simple problems, integration (which yields these results) of the applied loads directly in the equilibrium equations is preferred in general.

Next, let us consider internal forces and moments via the introduction of judicious cuts. Because of the uniform loading, however, one cut will suffice here. From Fig. 5.4c, we have for all $0 < x < L$,

$$\sum F_x = 0 \rightarrow f = 0,$$
$$\sum F_y = 0 \rightarrow q_o L - \int_0^x q_o dx - V = 0,$$

or $V(x) = q_o(L - x)$. Similarly,

$$\sum M_z\big)_A = 0 \rightarrow \frac{q_o L^2}{2} - \int_0^x q_o x\, dx - Vx + M_z = 0,$$

or

$$M_z(x) = Vx + \frac{q_o}{2}\left(x^2 - L^2\right)$$

where V is known from above; thus,

$$M_z(x) = q_o(L - x)x + \frac{q_o}{2}\left(x^2 - L^2\right).$$

Given these two results, we can now plot the desired shear and bending moment diagrams. First, however, let us observe an alternate but equivalent approach. Instead of the direct approach of cutting a beam and determining the internal shear forces and bending moments at a section by statics, an efficient alternative procedure can be used if the distributed external force $q(x)$ is known and integrated easily. Recall the basic differential equations derived earlier, namely Eqs. (5.4) and (5.9):

$$\frac{dV}{dx} = -q(x) \quad \text{and} \quad \frac{dM_z}{dx} = V(x).$$

Integrating Eq. (5.4) yields the shear force V, whereas integrating Eq. (5.9) yields the bending moment M_z. These ordinary differential equations can be used to solve for the shear forces and bending moments in beam problems. Hence, consider the following example.

Example 5.3 Find $V(x)$ and $M_z(x)$ for the beam in Example 5.2 using the governing ordinary differential equations, where $q(x) = q_o$.

Solution: By Eq. (5.4),

$$\frac{dV(x)}{dx} = -q_o \rightarrow \int \frac{d}{dx}(V(x))dx = -\int q_o\, dx,$$

or

$$V(x) = -q_o x + c_1.$$

By Eq. (5.9), we have

$$\frac{dM_z(x)}{dx} = -q_o x + c_1 \rightarrow \int \frac{d}{dx}(M_z(x))dx = \int (-q_o x + c_1)dx,$$

or

$$M_z(x) = -\frac{q_o x^2}{2} + c_1 x + c_2.$$

Applying the boundary conditions for a *free end*, $V(x = L) = 0$ and $M_z(x = L) = 0$, we obtain

$$0 = -q_o L + c_1 \rightarrow c_1 = q_o L$$

and

$$0 = -\frac{q_o L^2}{2} + q_o L^2 + c_2 \rightarrow c_2 = -\frac{q_o L^2}{2}.$$

Therefore,

$$V(x) = -q_o x + q_o L \rightarrow V(x) = q_o(L - x)$$

and

$$M_z(x) = -\frac{q_o x^2}{2} + c_1 x + c_2 \rightarrow M_z(x) = q_o L x - \frac{q_o}{2}\left(x^2 + L^2\right).$$

These results are the same as found in the previous example, as they should be. The shear and bending moment diagrams are in Fig. 5.5.

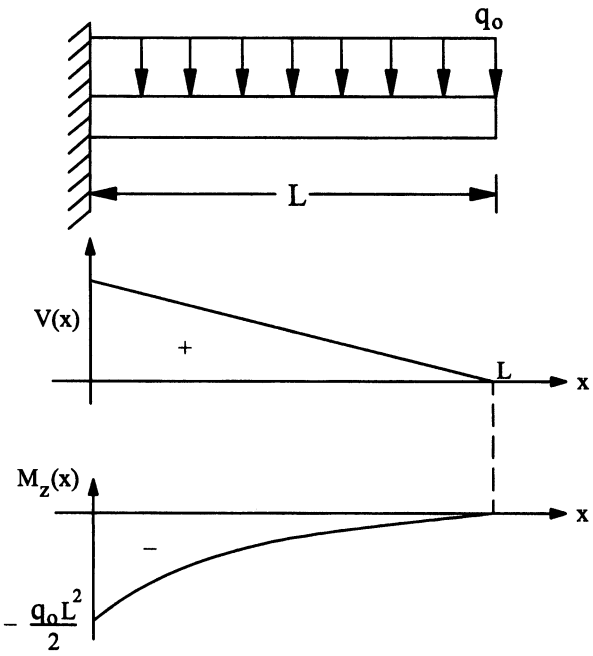

FIGURE 5.5 Shear and bending moment diagrams for the beam in Fig. 5.4.

5.2 Stresses in Beams

5.2.1 Biological Motivation

Recall from Chaps. 1 and 4 that it was probably first appreciated in bone that the local state of stress (or strain) influences greatly the underlying microstructure through growth and remodeling processes. Moreover, bone and teeth are among the few tissues in the body that exhibit elastic (and viscoelastic) behaviors under small strains. Finally, it is easily imagined that bones are routinely subjected to applied loads that tend to induce bending. A prime example is daily loading of the femur during walking and running because the line of action of the applied load does not go through the centroid of the diaphysis (see Figs. 4.1 and 4.7 as well as Sect. 3.3.2). Taken together, these observations reveal the importance of studying the bending of beams that exhibit a linear material behavior under small strains. Indeed, whether we are interested in understanding the maximum allowable transverse loads that an athlete's tibia or fibula can withstand without fracturing, designing a prosthesis for implantation, or studying mechanotransduction in osteoblasts and osteoclasts, knowledge of simple beam bending is of paramount importance.

5.2.2 Theoretical Framework

Despite the existence of specific examples that motivate the need to study particular problems, we emphasize that continuum mechanics is an approach to solving a broad class of problems; it is not a collection of specialized solutions. Recall from Chaps. 3 and 4, therefore, that in finding *the relation between stress and the applied loads and geometry* for the axially loaded rod, inflated thin-walled cylinders and spheres, and the torsion of a circular shaft, we first introduced a judicious cut to expose the stress of interest and then we enforced equilibrium (of the parts). Based on our examination of shear force and bending moment diagrams, it is clear that a fictitious cut will, in general, expose two types of stress: a normal stress σ_{xx} that serves to balance the moment M_z and a shear stress σ_{xy} that serves to balance the shear force V (Fig. 5.6). Nevertheless, let us begin our analysis by considering *pure bending*—bending in the absence of transverse loads and a σ_{xy} stress.

Normal Stress

To determine the normal stress in a beam subjected to pure bending, consider the differential element in Fig. 5.7 (in particular, note the assumed directions of loading). The forces in the x direction must balance, and so too the moments (i.e., externally applied and the internal resisting moments). Hence,

$$\sum F_x = 0 \rightarrow \int -\sigma_{xx} dA = 0 \tag{5.10}$$

and

$$\sum M_z)_A = 0 \rightarrow -M_z + \int y(-\sigma_{xx}) dA = 0. \tag{5.11}$$

Our two governing equilibrium equations are thus

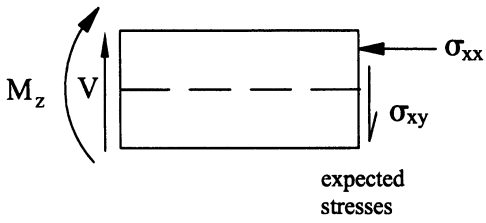

FIGURE 5.6 Schema of the need for x-face normal and shear stresses to balance a bending moment M_z and shear force V.

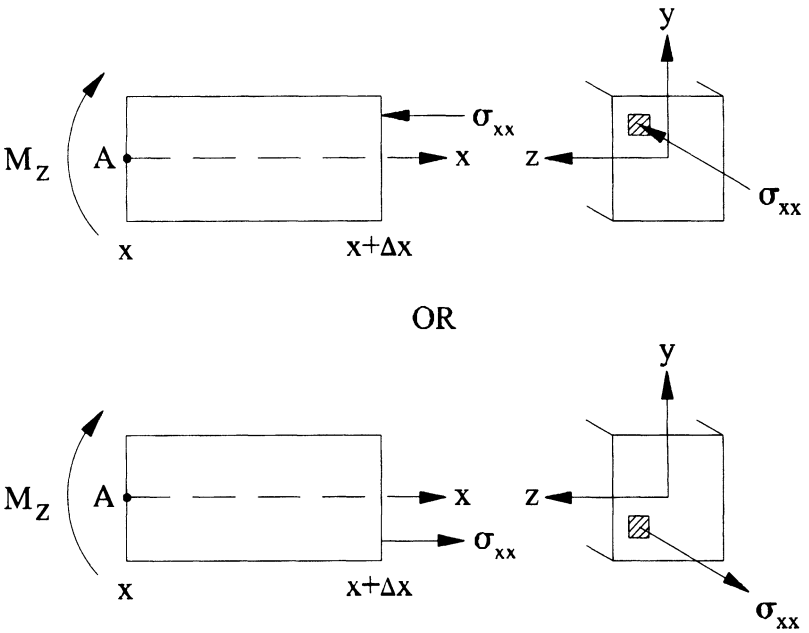

FIGURE 5.7 Side view and oblique view of a fictitiously cut beam that exposes the normal stress σ_{xx}, which acts over a differential area $dA = dydz$. Given the applied moment shown, the stress is expected to be compressive in the upper portion of the beam ($y > 0$) and tensile in the lower portion ($y < 0$). Either free-body diagram (*top* or *bottom*) is sufficient for purposes of a force balance.

$$\int -\sigma_{xx} dA = 0, \tag{5.12}$$

where $dA = dydz$ and

$$M_z = -\int y\sigma_{xx}\, dA, \tag{5.13}$$

the second of which relates the stress to the applied load (pure bending moment) and geometry (cross-sectional area). Similar to the torsion problem, however, the stress may vary in a yet unknown way: $\sigma_{xx} = \sigma_{xx}(y)$. Indeed, we expect a compressive stress in the upper portion of the cross section, where the (positive) bending moment tends to shorten the beam, and a tensile stress in the bottom portion, where the moment tends to lengthen the beam. Equation (5.12) requires that these compressive and tensile stresses must self-equilibrate.

As in the torsion problem, let us turn to kinematics and constitutive relations to find the function $\sigma_{xx}(y)$, which will allow us to integrate Eqs. (5.12) and

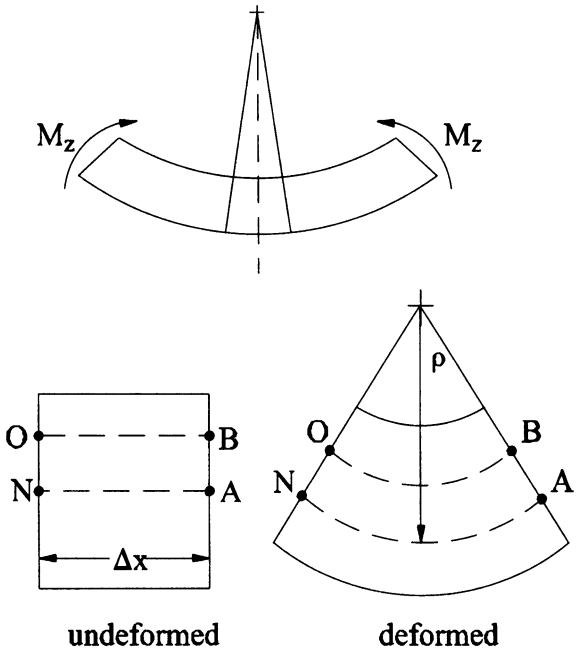

FIGURE 5.8 We assume that an initially straight beam subjected to a pure moment (i.e., no transverse loads) has a constant curvature at any depth (in the y direction). It will prove convenient, therefore, to consider line elements $\overline{OB}$ and $\overline{NA}$ in the x direction in both undeformed and deformed configurations. Furthermore, let the radius of curvature for the deformed line element $\overline{NA}$ be ρ. The arc length of $\overline{NA}$ is thus given by ρ times the subtended angle.

(5.13) as needed. Thus, consider the differential element extracted from Fig. 5.7 wherein we exaggerate the degree of bending (quantified by the radius of curvature ρ) to allow visualization (Fig. 5.8). Moreover, let us locate the coordinate system at the level wherein the width of the element is denoted $\overline{NA}$. Indeed, let us pick that level where $\overline{NA}$ equals the original width Δx; hence,

$$\overline{NA} = \Delta x = \rho \Delta \theta. \tag{5.14}$$

That one can find a location in the y direction where a line segment does not change length due to bending is revealed by the observation that line elements shorten in the compressive portion and lengthen in the tensile portion—somewhere between, one line segment must remain at a constant length, which thus serves as a convenient reference point.

Likewise, consider the line segment $\overline{OB}$, located a distance y above the level containing $\overline{NA}$. Whereas $\overline{OB} = \Delta x$ before deformation, after deformation we have

$$\overline{OB} = \Delta \theta (\rho - y). \tag{5.15}$$

The segment $\overline{OB}$ can also be rewritten in terms of Δx, which we prefer in light of Eqs. (5.4) and (5.9). From Eq. (5.14),

$$\overline{OB} = \Delta\theta(\rho - y) = \rho\Delta\theta - y\Delta\theta = \Delta x - y\frac{\Delta x}{\rho} = \Delta x\left(1 - \frac{y}{\rho}\right). \tag{5.16}$$

Recall from Chap. 2, therefore, that the linearized extensional strain can be thought of (over infinitesimal line segments) as

$$\varepsilon_{xx} = \frac{\text{Current length-Original length}}{\text{Original length}}. \tag{5.17}$$

Hence, the strain associated with the change in length of $\overline{OB}$ can be approximated as

$$\varepsilon_{xx} = \lim_{\Delta x \to 0} \frac{\Delta x(1 - y/\rho) - \Delta x}{\Delta x} = -\frac{y}{\rho} \to \varepsilon_{xx} = -\frac{y}{\rho}, \tag{5.18}$$

where the reciprocal of the radius of curvature ρ defines the curvature κ, with ρ and κ both constant with respect to x. It is important to note that if $y > 0$, then the strain is compressive, and if $y < 0$, then the strain is extensional, each consistent with the assumed compressive and tensile stresses σ_{xx} discussed earlier. Moreover, at $y = 0$ the strain is zero consistent with our selection of the location of $\overline{NA}$.

From Hooke's law for isotropic behavior [cf. Eq. (2.69)], $\sigma_{xx} = E\varepsilon_{xx}$ when $\sigma_{yy} = 0$ and $\sigma_{zz} = 0$, as assumed here. Hence, from Eq. (5.18),

$$\sigma_{xx} = E\left(-\frac{y}{\rho}\right). \tag{5.19}$$

Now, back to equilibrium, Eq. (5.12) becomes

$$\int -\left(-\frac{Ey}{\rho}\right) dA = 0 \to \frac{E}{\rho}\underbrace{\int y dA}_{\overline{y}A} = 0 \to \frac{EA}{\rho}\overline{y} = 0, \tag{5.20}$$

where $\overline{y}$ is the distance from the origin of our (x, y, z) coordinate system to the centroid of the cross-sectional area A (recall Eq. (A3.2)). Because this integral equals zero and the Young's modulus E, radius of curvature ρ, and cross-sectional area A are each nonzero, the distance $\overline{y}$ must be set equal to zero; that is, the z axis must pass through the centroid of the cross-section. This means that the coordinate system, at $\overline{NA}$, must be located at the centroid. Next, from Eq. (5.13),

$$-\int y\left(-\frac{Ey}{\rho}\right)dA = M_z \rightarrow \frac{E}{\rho}\underbrace{\int y^2 dA}_{I_{zz}} = M_z \tag{5.21}$$

wherein we recognize the second moment of area I_{zz} (Appendix 4 of Chap. 4), thus moment balance requires

$$M_z = \frac{EI_{zz}}{\rho}. \tag{5.22}$$

This equation is called *the moment-curvature relation*; it will prove critical in our subsequent discussion of beam deflections in Sect. 5.3. Here, however, note that by rearranging Eq. (5.22) and using Eq. (5.19), we obtain our desired relation for the normal stress in terms of the applied load and geometry:

$$\sigma_{xx} = -\frac{M_z(x)y}{I_{zz}}. \tag{5.23}$$

This equation is called the *flexure formula*; it is one of the most important relations in elementary solid mechanics. Before we explore its use, however, let us observe the following. In bending, the locus of all centroids is called the *neutral axis*, $\overline{NA}$, for it is where $\varepsilon_{xx} = -y/\rho$ and $\sigma_{xx} = -M_z y/I_{zz}$ both equal zero (i.e., are neutral). The neutral axis for any elastic beam of homogeneous composition can thus be determined easily by finding the centroid of the cross-sectional area of the beam.

Finally, Eq. (5.23) allows us to compute the normal stress σ_{xx} at any x [due to $M_z(x)$ dependence] or y; we assume that σ_{xx} does not vary with z. Because of our small strain, small slope of the deflection curve, and use of Hooke's law, this flexure formula is not a universal result; it is restricted to small-strain LEHI behavior. Let us now consider the case in which transverse loads exist, which give rise to shear stresses σ_{xy}.

Shear Stress

Whereas we derived the flexure formula for σ_{xx} due to pure bending (moment only), we will assume that the same formula [Eq. (5.23)] holds equally well for bending due to transverse loads and that this stress can be considered simultaneously with other stresses that arise from the transverse loads. This is tantamount to assuming a superposition of solutions in a linear problem as we did when considering combined internal pressurization and axial loading of a thin-walled cylinder.

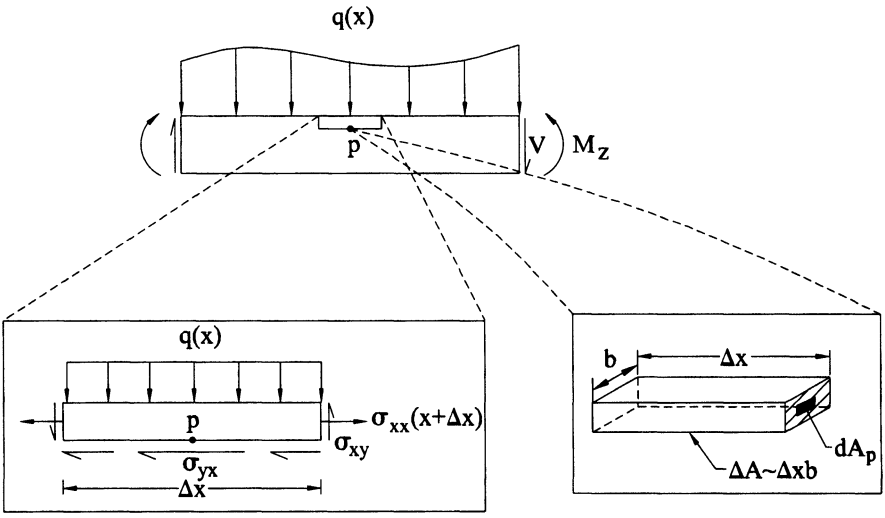

FIGURE 5.9 Consider a small rectangular portion of a beam taken above point p and on which σ_{yx} shear stresses act on the bottom y face; recalling the requirement from angular momentum balance that the stress be symmetric (i.e., $\sigma_{xy} = \sigma_{yx}$), this is consistent with the need for σ_{xy} shear stresses on the x face to balance the transverse loads. Note that the shear stress is shown according to its standard positive sign convention, not for the adopted positive sign convention for the shear force in Fig. 5.6; note, too, that we neglect σ_{yy} in general and thus require σ_{xy} to balance all of the vertical load.

In the presence of transverse loads, we must also account for the shear stresses that act to balance V (Fig. 5.6). Here, therefore, let us derive a general relation that relates the shear stress σ_{xy} to the applied load and geometry. Hindsight reveals that an approach different from that used to derive σ_{xx} (wherein we used the sum of the effects of all σ_{xx} stresses acting over their differential areas to balance directly the applied bending moment) will prove useful. Hence, consider the following.

Let us extract a small rectangular piece of a generic beam as shown in Fig. 5.9 such that we expose the stresses σ_{yx} at the point p (i.e., in the limit as $\Delta x \to 0$) Moreover, whereas we must ensure force balance in x and y as well as moment balance, here we shall focus only on force balance in x. Note, therefore, that

$$\sum F_x = 0 \to -\int \sigma_{xx}(x)dA + \int \sigma_{xx}(x + \Delta x)dA - \int \sigma_{yx}dA_s = 0, \qquad (5.24)$$

where dA_s simply denotes the area over which the shear stress σ_{yx} acts, and consistent with our approach in the previous section,

$$\sigma_{xx}(x) = -\frac{M_z y}{I_{zz}}, \qquad \sigma_{xx}(x+\Delta x) = -\frac{(M_z + \Delta M_z) y}{I_{zz}}. \tag{5.25}$$

Hence, we see that force balance requires

$$+\frac{M_z}{I_{zz}}\int y\, dA_p - \frac{M_z}{I_{zz}}\int y\, dA_p - \frac{\Delta M_z}{I_{zz}}\int y\, dA_p - \int \sigma_{yx}\, dA_s = 0. \tag{5.26}$$

Noting that the first two terms cancel and that the $\int y dA_p$ is *the first moment of area for the exposed cross section above point p*, we have

$$-\frac{\Delta M_z}{I_{zz}} Q = \int \sigma_{yx}\, dA_s, \tag{5.27}$$

where, for notational simplicity, we let $Q = \int y dA_p$. Finally, note that to complete the derivation, we must either consider the average value of σ_{yx} (as in the thin-walled tube problem) or find how σ_{yx} varies with x so that we can integrate over $dA_s = dxdz$. Knowing that we seek to shrink Δx to a point in the limit and assuming that σ_{yx} does not vary with z (similar to our implicit assumption for σ_{xx}), we can write

$$-\frac{\Delta M_z}{I_{zz}} Q = \sigma_{yx}\big)_{\text{ave}}\, \Delta x b \rightarrow \sigma_{yx}\big)_{\text{ave}} = -\frac{\Delta M_z}{\Delta x}\left(\frac{Q}{I_{zz} b}\right), \tag{5.28}$$

which in the limit becomes

$$\sigma_{yx}\big)_{\text{ave}} = -\frac{dM_z}{dx}\left(\frac{Q}{I_{zz} b}\right), \tag{5.29}$$

whereby we recall from Eq. (5.9) that $V(x) = dM_z/dx$. Our derivation is thus complete except for one observation. Note that we denoted σ_{yx} and σ_{xy} on the isolated part of the beam according to our general sign convention for stress (cf. Fig. 2.4). We must be consistent with our sign convention for $V(x)$ and $M_z(x)$ for beam bending, whereby we defined a positive $V(x)$ on a positive x face to be in the negative direction (cf. Fig. 5.1). Hence, just as in statics, when we obtain a negative value in an analysis, this tells us that our quantity acts opposite to the direction assumed. Thus, the negative sign in Eq. (5.29) tells us that $\sigma_{yx})_{\text{ave}}$ acts opposite to the direction assumed and so too for σ_{xy}, which is numerically equal to σ_{yx} at a point due to moment balance [Eq. (2.7)]. Hence, given these observations, we have the desired result

$$\sigma_{xy)\text{ave}} = \left(\frac{V(x)Q(y)}{I_{zz}b}\right), \tag{5.30}$$

where $Q = \int y dA_p$ and b is the width of the beam at point p where the stress is evaluated. Note, too, that $\sigma_{xy)\text{ave}}$ acts in the direction of the shear $V(x)$ and that this relation relates the stress to the applied shear force and geometry (measures being Q, I_{zz}, and b). Knowing that σ_{xy} is an average value over b, we will drop the notation $\sigma_{xy)\text{ave}}$ and simply write σ_{xy}.

As a final observation, note that because Q is a first moment of area, it can be computed simply as (recall Appendix 3 of Chap. 3)

$$Q = \overline{y}_p A_p, \tag{5.31}$$

where $\overline{y}_p$ locates the centroid of the cross-sectional area *above* point p relative to the overall centroid, and A_p is the area above point p. To better appreciate this, consider the following example.

Example 5.4 Find the value of Q for the rectangular cross section in Fig. 5.10 at the following points $y = h/2$, $h/4$, 0, $-h/4$, $-h/2$, three of which are emphasized in the figure.

Solution: Here, it will prove useful to compute $Q = \overline{y}_p A_p$ for each point of interest and to do so in tabular form.

y-Location of p	$\overline{y}_p$	A_p	Q
$\frac{h}{2}$	$\frac{h}{2}$	0	0
$\frac{h}{4}$	$\frac{h}{4}+\frac{h}{8}$	$\frac{h}{4}b$	$\frac{3}{32}bh^2$
0	$\frac{h}{4}$	$\frac{h}{2}b$	$\frac{1}{8}bh^2$
$-\frac{h}{4}$	$\frac{h}{8}$	$\frac{3h}{4}b$	$\frac{3}{32}bh^2$
$-\frac{h}{2}$	0	hb	0

From this example, therefore, we see that Q varies with y, being smallest (zero) at the top and bottom and largest at the overall centroid. Indeed, for the simple case of a rectangular cross section, we can obtain a general formula for Q, namely

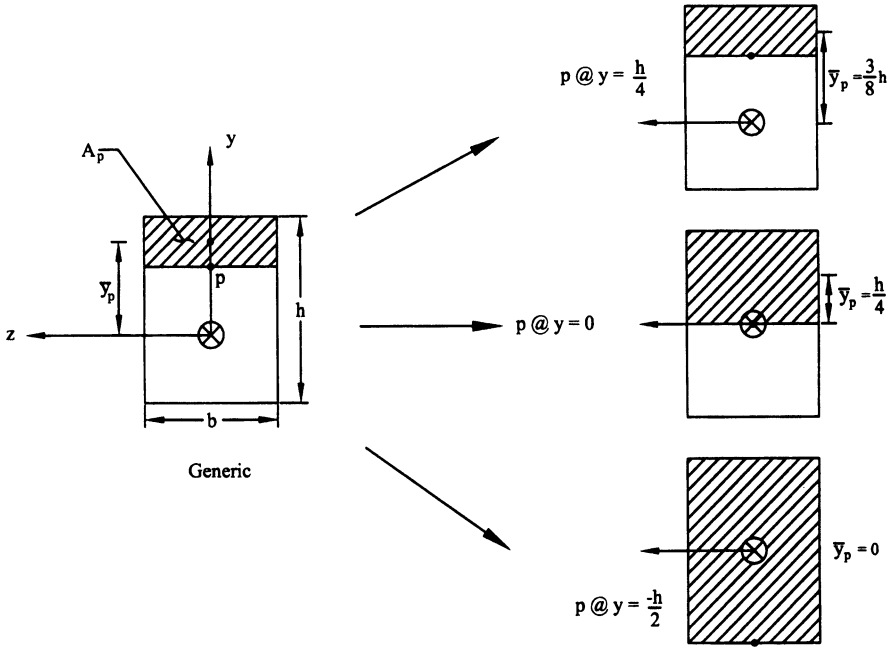

FIGURE 5.10 Illustration of the method for determining the value of $Q = \bar{y}_p A_p$ in a rectangular cross section. The subscript p reminds us that these quantities are defined for the cross-sectional areas above a point p rather than over the entire cross section. Forgetting this is a common error. Q is seen to be zero at the top and bottom surfaces for different reasons.

$$Q = \int_{-b/2}^{b/2} \int_{y}^{h/2} y\,dy\,dz = b\left(\frac{1}{2}y^2 \middle| \begin{matrix} h/2 \\ y \end{matrix}\right) = \frac{b}{2}\left(\frac{h^2}{4} - y^2\right), \tag{5.32}$$

which we see recovers the results in the above table. In this case, Q varies quadratically with the location of interest p in the y direction. From the relation $\sigma_{xy} = VQ/I_{zz}b$, therefore, we see that the shear stress would likewise vary quadratically with y, being zero on the top and bottom surfaces but largest at the centroid. This is in contrast to the normal stress $\sigma_{xx} = -M_z y/I_{zz}$, which varies linearly with y and is zero at the centroid and largest at the top and bottom surfaces. The stress field in a beam subject to bending will thus be complex in general.

Question: Does it make sense that σ_{xy} is zero at values of y that correspond to the top and bottom surfaces? To answer this question, it is useful to recall two things. First, $\sigma_{xy} = \sigma_{yx}$ at any point due to moment balance as revealed in Chap. 2. Second, we are only considering beams that are subjected to bending

moments or transverse loads. Hence, there are no x-directed forces on the top and bottom y faces and thus no σ_{yx} $(=\sigma_{xy})$ stresses on these faces. Thus, our result for $\sigma_{xy} = VQ/I_{zz}b$ does make sense on these top and bottom surfaces.

Finally, although our approach for deriving the relation for σ_{xy} differed from the direct force balance used to derive the flexure formula for σ_{xx}, force balance must be respected nonetheless. Hence, consider the following example.

Example 5.5 Show that $\int \sigma_{xy} dA = V$ at any x.

Solution: Although the result can be obtained more generally, let us consider the rectangular cross section in Fig. 5.10. Using Eq. (5.30), we have

$$\int \sigma_{xy}\, dA = \int_{-b/2}^{b/2} \int_{-h/2}^{h/2} \frac{V(x)Q(y)}{I_{zz}b}\, dy\, dz = \frac{V}{I_{zz}b} \int_{-b/2}^{b/2} dz \int_{-h/2}^{h/2} Q(y)\, dy$$

which from Eq. (5.32) can be written as

$$\int \sigma_{xy}\, dA = \frac{V}{I_{zz}} \int_{-h/2}^{h/2} \frac{b}{2}\left(\frac{h^2}{4} - y^2\right) dy,$$

where $I_{zz} = (\mathrm{l}/12)bh^3$ for the rectangular cross section. Hence,

$$\int \sigma_{xy}\, dA = \frac{12V}{bh^3}\left(\frac{b}{2}\right)\left(\frac{h^2}{4}y - \frac{1}{3}y^3 \Bigg|_{-h/2}^{h/2}\right) = \frac{6V}{h^3}\left[\frac{h^2}{4}\left(\frac{h}{2} + \frac{h}{2}\right) - \frac{1}{3}\left(\frac{h^3}{8} + \frac{h^3}{8}\right)\right]$$
$$= \frac{6V}{h^3}\left(\frac{h^3}{4} - \frac{h^3}{12}\right) = V,$$

which proves that vertical force balance is respected in this case, as it should.

Principal Values and Maximum Shear

If we want to find maximum normal stress or maximum shear stress (at each point), we recall from Chap. 2 that

$$\sigma'_{xx})_{\max/\min} = \frac{\sigma_{xx} + \sigma_{yy}}{2} \pm \sqrt{\left(\frac{\sigma_{xx} - \sigma_{yy}}{2}\right)^2 + \sigma_{xy}^2} \tag{5.33}$$

and

$$\sigma'_{xx})_{\max/\min} = \pm\sqrt{\left(\frac{\sigma_{xx}-\sigma_{yy}}{2}\right)^2 + \sigma_{xy}^2}. \tag{5.34}$$

For beam bending, these equations for the maximum values become

$$\sigma'_{xx})_{\max} = -\frac{M_z(x)y}{2I_{zz}} \pm \sqrt{\left(-\frac{M_z(x)y}{2I_{zz}}\right)^2 + \left(\frac{V(x)Q(y)}{I_{zz}\,b}\right)^2} \tag{5.35}$$

$$\sigma'_{xy})_{\max} = \sqrt{\left(-\frac{M_z(x)y}{2I_{zz}}\right)^2 + \left(\frac{V(x)Q(y)}{I_{zz}\,b}\right)^2}, \tag{5.36}$$

where each varies with (x, y) in general. Let us now consider a few illustrative examples.

5.2.3 *Illustrative Examples*

Example 5.6 Find σ_{xx}, the maximum normal stress $\sigma'_{xx})_{\max}$, and the maximum shear stress $\sigma'_{xy})_{\max}$ for the beam in Fig. 5.11 with an applied bending moment M_o. Neglect the weight of the beam.

Solution: A free-body diagram of the whole structure reveals that we have

$$\sum F_x = 0 \rightarrow R_x = 0,$$
$$\sum F_y = 0 \rightarrow R_y = 0,$$
$$\sum M_z)_B = 0 \rightarrow M_o - M_w - R_y L = 0,$$

and, thus,

$$M_w = M_o.$$

A free-body diagram of part of the beam similarly requires

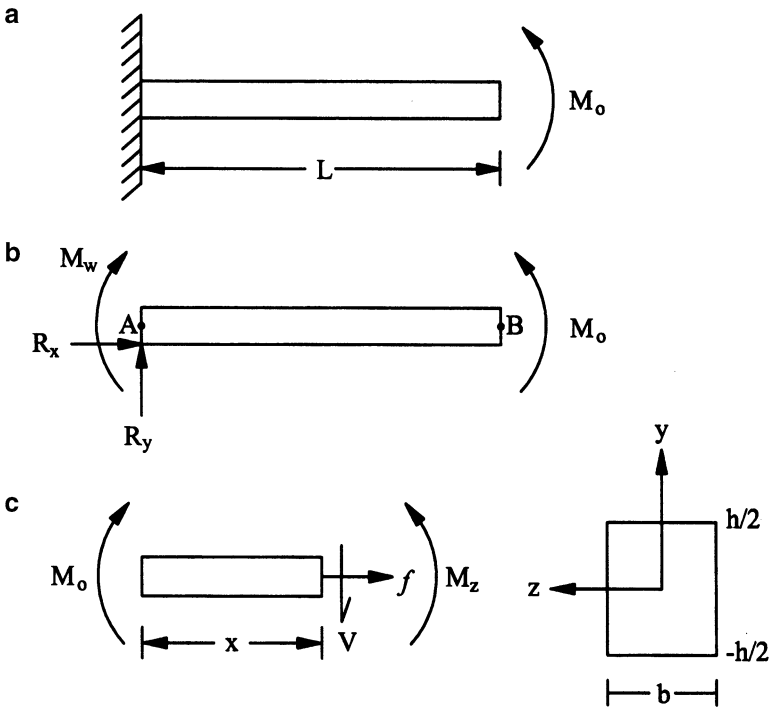

FIGURE 5.11 A cantilever beam having a rectangular cross section and subjected to an applied moment at the end. Free-body diagrams of the whole and the parts isolate reaction and internal forces and moments as needed. One cut is sufficient because the loads are applied only at the ends.

$$\sum F_x = 0 \rightarrow f = 0,$$
$$\sum F_y = 0 \rightarrow V(x) = 0 \quad \forall x$$
$$\sum M_z)_A = 0 \rightarrow -M_o + M_z(x) - Vx = 0,$$

and thus, as expected,

$$M_z(x) = M_o.$$

Next, we could draw the shear force and bending moment diagrams, which are trivial in this case of pure bending. From Eq. (5.23), therefore, we have

$$\sigma_{xx} = -\frac{M_0 y}{I_{zz}} \quad \forall x \in [0, L],\ y \in \left[-\frac{h}{2}, \frac{h}{2}\right],\ z \in \left[-\frac{b}{2}, \frac{b}{2}\right],$$

where

$$I_{zz} = \int y^2\, dA = \int_{-b/2}^{b/2} \int_{-h/2}^{h/2} y^2\, dy\, dz = \int_{-b/2}^{b/2} \frac{h^3}{12} dz = \frac{h^3 b}{12}.$$

Because σ_{xx} balances the applied load at each cross section, there is no need for any other component of stress relative to (x, y, z). The largest compressive and tensile loads, relative to (x, y, z), occur at $y = \pm h/2$; hence,

$$\sigma_{xx}\left(y = \pm\frac{h}{2}\right) = \mp\frac{12M_o}{bh^3}\left(\frac{h}{2}\right) = \mp\frac{6M_o}{bh^2}.$$

Considering only a 2-D state of stress here (e.g., σ_{xx}, σ_{yy}, and $\sigma_{xy} = \sigma_{yx}$), we recall from Chap. 2 that the maximum/minimum normal stresses are called principal stresses. They are computed via

$$\sigma'_{xx})_{\substack{\max \\ \min}} = \frac{\sigma_{xx} + \sigma_{yy}}{2} \pm \sqrt{\left(\frac{\sigma_{xx} - \sigma_{yy}}{2}\right)^2 + \sigma_{xy}^2},$$

where $\sigma_{yy} = 0 = \sigma_{xy}$. Using the largest value of σ_{xx} (i.e., at $y = h/2$), we find that

$$\sigma'_{xx})_{\max} = \frac{\sigma_{xx}}{2} + \sqrt{\frac{\sigma_{xx}^2}{4}} = \frac{6M_o}{bh^2},$$

$$\sigma'_{xx})_{\min} = \frac{\sigma_{xx}}{2} - \sqrt{\frac{\sigma_{xx}^2}{4}} = 0.$$

Hence, x and y are principal directions ($\alpha_p = 0$).

The maximum/minimum shear stress, however, is

$$\sigma'_{xy})_{\substack{\max \\ \min}} = \pm\sqrt{\left(\frac{\sigma_{xx} - \sigma_{yy}}{2}\right)^2 + \sigma_{xy}^2} = \pm\frac{\sigma_{xx}}{2}$$

and, therefore,

$$\sigma'_{xy})_{\substack{\max \\ \min}} = \pm\frac{3M_o}{bh^2},$$

which occurs at $\alpha_s = \pi/4$ or 45° and $y = \pm h/2$, not at $y = 0$ (the centroid), where σ_{yx} is largest in general. We see, therefore, that we must pay particularly close attention to the coordinate system to which quantities are referred as well as possible failure mechanisms (e.g., ductile materials yield in response to shear stresses and brittle materials fracture in response to normal stresses).

Example 5.7 Find general relations for σ_{xx} and σ_{xy} in terms of P, x, y, b, and $\overline{y}_p$ for the beam shown in Fig. 5.12. Next find the values of each of these components of stress at the following (x, y) locations: $(0, h/2)$, $(0, 0)$, $(L/2, h/2)$, $(L/2, 0)$, $(L, h/2)$, $(L, 0)$, $(L, -h/2)$.

Solution: From the free-body diagram of the whole structure, we see that

$$\begin{aligned} \sum F_x = 0 &\rightarrow R_x = 0, \\ \sum F_y = 0 &\rightarrow R_y = P, \\ \sum M_z)_A = 0 &\rightarrow -M_A - PL = 0, \\ M_A &= -PL. \end{aligned}$$

Next, let us find the internal forces and moments. From a free-body diagram of the parts, we obtain

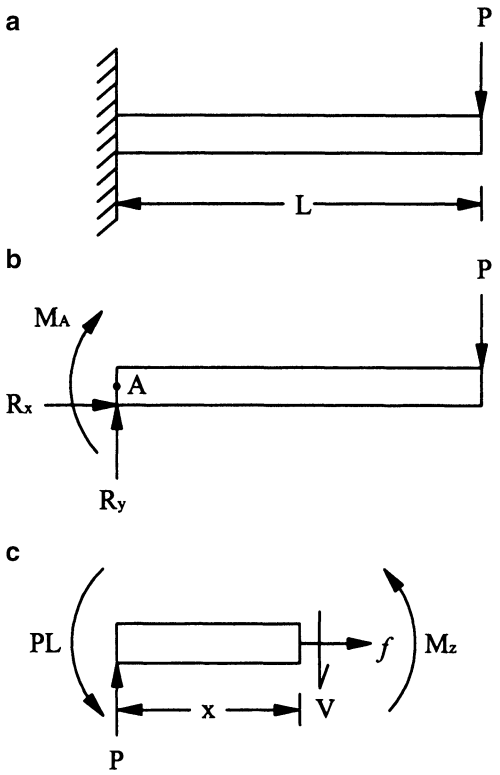

FIGURE 5.12 Similar to Fig. 5.11 except for a cantilever beam having a rectangular cross section and subjected to an applied transverse load P at the end.

$$\sum F_x = 0 \rightarrow f = 0,$$
$$\sum F_y = 0 \rightarrow V = P,$$
$$\sum M_z\big)_A = 0 \rightarrow PL - Vx + M_z = 0,$$
$$M_z = Vx - PL = P(x - L).$$

From Eq. (5.23), therefore,

$$\sigma_{xx} = -\frac{M_z y}{I_{zz}} = -\frac{P(x-L)y}{I_{zz}} \quad \forall x, y, z,$$

where

$$I_{zz} = \int_{-b/2}^{b/2}\int_{-h/2}^{h/2} y^2\, dy\, dz = \frac{1}{12}bh^3.$$

From Eq. (5.30),

$$\sigma_{xy}\big)_{\text{ave}} = \frac{VQ}{I_{zz}b} = \frac{PQ}{I_{zz}b},$$

where

$$Q = \int y\, dA_p = \int_{-b/2}^{b/2}\int_{y}^{h/2} y\ dy\ dz = \int_{-b/2}^{b/2}\left(\frac{h^2}{8} - \frac{y^2}{2}\right)dz = \frac{b}{2}\left(\frac{h^2}{4} - y^2\right).$$

Hence,

$$\sigma_{xx} = \frac{12P(x-L)y}{bh^3} \quad \text{and} \quad \sigma_{xy} = \frac{12P\left[b\left(h^2/4 - y^2\right)/2\right]}{b^2h^3}.$$

Now, we can compute σ_{xx} and σ_{xy} at various points of interest p. For example, for the points indicated, let the point $(x, y) = (0, h/2)$; $(0, 0)$; $(L/2, h/2)$; $(L/2, 0)$; $(L, h/2)$; $(L, 0)$; $(L, -h/2)$.

(x, y)	σ_{xx}	σ_{xy}
$\left(0, \frac{h}{2}\right)$	$-\frac{P(0-L)(h/2)}{(1/12)bh^3} = \frac{6PL}{bh^2}$	$\frac{P\left[(b/2)\left(h^2/4 - (h/2)^2\right)\right]}{(1/12)b^2h^3} = 0$
$(0, 0)$	$-\frac{P(0-L)0}{(1/12)bh^3} = 0$	$\frac{P\left[(b/2)\left(h^2/4 - 0^2\right)\right]}{(1/12)b^2h^3} = \frac{3P}{2bh}$

(continued)

(x, y)	σ_{xx}	σ_{xy}
$\left(\frac{L}{2}, \frac{h}{2}\right)$	$-\frac{P(L/2-L)(h/2)}{(1/12)bh^3} = \frac{3PL}{bh^2}$	$\frac{P\left[(b/2)\left(h^2/4-(h/2)^2\right)\right]}{(1/12)b^2h^3} = 0$
$\left(\frac{L}{2}, 0\right)$	$-\frac{P(L/2-L)0}{(1/12)bh^3} = 0$	$\frac{P\left[(b/2)\left(h^2/4-0^2\right)\right]}{(1/12)b^2h^3} = \frac{3P}{2bh}$
$\left(L, \frac{h}{2}\right)$	$-\frac{P(L-L)(h/2)}{(1/12)bh^3} = 0$	$\frac{P\left[(b/2)\left(h^2/4-(h/2)^2\right)\right]}{(1/12)b^2h^3} = 0$
$(L, 0)$	$-\frac{P(L-L)0}{(1/12)bh^3} = 0$	$\frac{P\left[(b/2)\left(h^2/4-0^2\right)\right]}{(1/12)b^2h^3} = \frac{3P}{2bh}$
$\left(L, -\frac{h}{2}\right)$	$-\frac{P(L-L)(-h/2)}{(1/12)bh^3} = 0$	$\frac{P\left[(b/2)\left(h^2/4-(h/2)^2\right)\right]}{(1/12)b^2h^3} = 0$

Whereas we have determined the values of the components σ_{xx} and σ_{xy} at the indicated points, we emphasize that σ_{xx} and σ_{xy} can (should) be found at all (x, y). Indeed, at each (x, y), we should also compute the maximum normal stress $\sigma'_{xx})_{\max}$ if we expect failure to occur due to normal stresses (e.g., in brittle materials) or the maximum shear stress $\sigma'_{xy})_{\max}$ if we expect failure to occur in shear (e.g., in ductile materials). Because the principal and maximum shear stresses both depend on σ_{xx} and σ_{xy}, it is clearly more challenging to identify the point in the structure where an absolute maximum stress exists. For this reason and given the availability of computers and color graphics, many simply create color contour plots of the principal or maximum shear stresses to aid failure analysis.

At this juncture, we should emphasize that we have neglected the σ_{yy} component of stress. Clearly, in response to transverse loads applied to the top or bottom surfaces $y = \pm h/2$, σ_{yy} stresses will exist. Indeed, in the case of a concentrated load P (Fig. 5.13), the σ_{yy} stress can be very large close to the applied load. Inclusion of such effects generally requires numerical methods, however, and thus are beyond the present scope. Because real loads are applied over finite, not infinite, areas and because σ_{xx} and σ_{xy} tend to dominate, we will focus on these components throughout.

Observation 5.1. Although we have ignored potential "stress concentrations" due to concentrated transverse loads in our simple beam theory, the issue of stress concentrations is nevertheless very important in mechanics. Basically, a *stress concentration* can arise due to an abrupt change in geometry, material

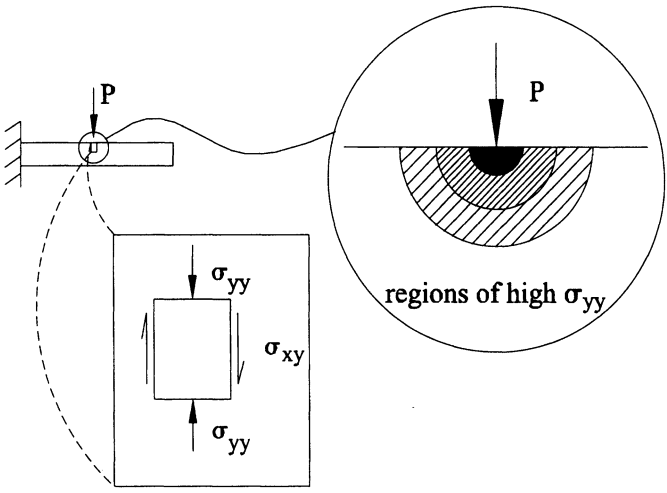

FIGURE 5.13 Schema of y-face, y-direction stresses σ_{yy} in the neighborhood of a concentrated load P. The *contour lines* show that the value of σ_{yy} decreases (shown by cross-hatching that becomes less dense) as one gets farther from the source of the concentrated load. No real load is truly concentrated, of course, for it must act over a finite, albeit possibly small, area.

properties, or applied load; it is characterized by a significantly increased value of stress locally, with associated steep gradients with respect to stresses in the surrounding area. Stress concentrations may arise at holes, sharp edges, interfaces between materials of dissimilar stiffness, and, of course, at concentrated loads. Hence, methods to combat the potentially deleterious effects of stress concentrations include rounding edges, functionally grading the stiffness of a material (e.g., a metallic intravascular stent), and distributing a load over a broader area. Because stress concentrations are characterized by steep gradients in stress, analytic solutions are often not possible. One must often resort to numerical methods, such as finite elements, or perhaps experimental methods, such as photoelasticity. Fortunately, many general problems have been solved and categorized for reference. For example, see Roark and Young (1975) wherein stress concentration factors are given for many geometries. A stress concentration factor K is defined simply as a ratio of the maximum expected stress to the mean stress in that region (e.g., $\sigma_{\max} = K\sigma_{\text{avg}}$), typically in reference to normal stresses. For example, in a LEHI material, the stress in a uniaxially loaded member is higher near a centrally placed hole by a factor of 2–3 depending on the ratio of the radius of the hole a to the width of the uniaxial sample d: $K = 3$ if $2a/d \sim 0$, but $K = 2$ if $2a/d \sim 1$. Holes are introduced in skin by dermatologists when taking a skin biopsy, in the lens capsule of the eye by ophthalmologists when implanting an intraocular device, in bone when an orthopedic surgeon puts in a bone screw, and so on. Understanding the effects

of stress concentrations is thus very important in biomechanics even though our discussion here is very brief.

5.3 Deformation in Beams

5.3.1 Biological Motivation

Mechanics is the study of motions and the applied loads that cause them. Fundamental to the study of beams, therefore, is the quantification of strains and deflections. For example, if we seek to quantify the material parameters of Hooke's law for bone, we must know both stresses and strains at representative points. Likewise, recall from Chap. 3 that one type of failure can be excessive deformation. Hence, if we are to design an orthotic device to maintain two ends of a severely fractured bone in close proximity during the healing process, we must ensure that the orthotic device does not deform excessively under loads experienced during daily activity. Indeed, as we will see, measuring or computing deformations in beams is extremely important in many different situations in biomechanics.

5.3.2 Theoretical Framework

Recalling from the definition of Poisson's ratio that $v = -\varepsilon_{\text{transverse}}/\varepsilon_{\text{axial}}$, Eq. (5.18) yields

$$v = -\frac{\varepsilon_{yy}}{\varepsilon_{xx}} \rightarrow \varepsilon_{yy} = -v\left(-\frac{y}{\rho}\right) = v\left(\frac{y}{\rho}\right). \tag{5.37}$$

The "same" relation holds for ε_{zz} because

$$\varepsilon_{yy} = \frac{1}{E}\left[\sigma_{yy} - v(\sigma_{xx} + \sigma_{zz})\right] = -\frac{v}{E}\sigma_{xx} \tag{5.38}$$

and

$$\varepsilon_{zz} = \frac{1}{E}\left[\sigma_{zz} - v\left(\sigma_{xx} + \sigma_{yy}\right)\right] = -\frac{v}{E}\sigma_{xx}. \tag{5.39}$$

Hence, because the Poisson's ratio v is typically non-negative, the beam widens in z where it shortens in x ($y > 0$ for $M_z > 0$) and it narrows in z where it lengthens in x ($y < 0$ for $M_z > 0$). This phenomenon is called *anticlastic* bending. Note: the Greek nu used to denote Poisson's ratio appears similar to the Latin v used below for deflection. The correct variable is obvious given the context.

Finally, to get more information on the deformation, recall the moment-curvature relation, [Eq. (5.22)], which we now write as

$$\frac{1}{\rho} = \frac{1}{EI_{zz}} M_z. \tag{5.40}$$

Recall, too, from calculus that the curvature κ is defined as

$$\kappa = \frac{1}{\rho} = \frac{d^2v/dx^2}{\sqrt[3]{1 + (dv/dx)^2}} \tag{5.41}$$

where $v(x)$ denotes the vertical *deflection* of the neutral axis (i.e., v is a vertical displacement u_y of points along the neutral axis only). Clearly then, if we let $dv/dx \ll 1$ [i.e., if we consider beam deflections $v = v(x)$ having small slopes], then

$$\frac{1}{\rho} \cong \frac{d^2v}{dx^2}. \tag{5.42}$$

By substituting this result into the moment-curvature relation, we obtain a general differential equation for the beam deflection:

$$EI_{zz} \frac{d^2v}{dx^2} = M_z(x). \tag{5.43}$$

In summary, Eq. (5.18) allows us to compute the extensional strain ε_{xx} at any location y provided that we know the radius of curvature ρ, which is evaluated at the neutral axis $\overline{NA}$. Equation (5.43) similarly provides information on the deflection $v(x)$ of the neutral axis given information on the applied load $M_z(x)$, geometry I_{zz}, and material property E. Compare this to the results for axial extension δ and rotation Θ in the axial load and torsion problems, respectively.

Because Eq. (5.43) is a second-order differential equation, we will need two boundary conditions for its full solution. These conditions will be on either the deflection v at a particular value of x or the slope dv/dx at a particular x. Recall, therefore, that the deflection v will be zero at a pin or a fixed end; the deflection at a roller is zero if the beam is pushed toward the roller. In contrast, a free end or an end on a slider cannot resist a deflection (Fig. 5.14). Conversely, the slope dv/dx is zero at a fixed end or a slider, but it cannot be specified at a roller, a pin, or a free end. An easy way to remember these *kinematic* boundary conditions is to remember the associated *traction* boundary conditions; that is, to restrict a vertical deflection, the support must be able to supply a resisting vertical reaction force R_y, and to restrict a rotation (i.e., a slope), the support must be able to supply a resisting bending moment M_z.

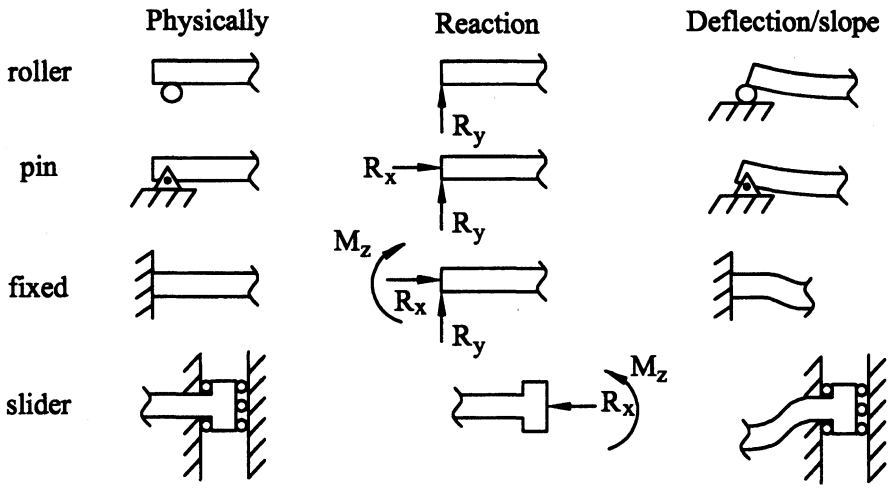

FIGURE 5.14 Possible boundary conditions for various supports showing both the reactions and the possible motions. Note that an applied force is capable of preventing (or limiting) a displacement in the same direction, whereas an applied moment is capable of preventing (or limiting) a rotation. Thus, one can prescribe at a support either an applied load or the resulting motion, but not both.

Let us note that Eqs. (5.4) and (5.9), in combination with Eq. (5.43), allow us to formulate alternative differential equations for the deflection curve $v(x)$; that is,

$$\frac{dM_z}{dx} = V(x) \rightarrow \frac{d}{dx}\left(EI_{zz}\frac{d^2v}{dx^2}\right) = V(x) \tag{5.44}$$

or

$$\frac{dV}{dx} = -q(x) \rightarrow \frac{d^2}{dx^2}\left(EI_{zz}\frac{d^2v}{dx^2}\right) = -q(x). \tag{5.45}$$

If the beam is of constant cross section and E does not vary with x, we see further that these third- and fourth-order differential equations can be written as

$$EI_{zz}\frac{d^3v}{dx^3} = V(x) \quad \text{and} \quad EI_{zz}\frac{d^4v}{dx^4} = -q(x). \tag{5.46}$$

In a given problem, therefore, we have the option to solve any *one* of the governing differential equations. The choice of which equation to attempt to solve should be dictated by our knowledge of the loading functions, $M_z(x)$, $V(x)$ or $q(x)$ as well as boundary conditions. Indeed, the higher-order equations require us to know moments or shears at the boundaries. At a "free end," for example, the

moment or shear will be that which is applied; if it is truly a free end, with no physical support or applied load, we will have zero moment and zero shear. Various boundary conditions will be examined in the following examples.

5.3.3 Illustrative Examples

Example 5.8 Find the deflection curve of the beam in Example 5.6

Solution: Let $v(x)$ be the deflection curve (i.e., shape of the neutral axis in the deformed configuration). Recalling the governing differential equation $EI_{zz}d^2v/dx^2 = M_z(x)$ from Eq. (5.43) and that $M_z(x) = M_o$ for this beam, integrating once yields an expression for the slope of the deflection curve:

$$\int \frac{d}{dx}\left(\frac{dv(x)}{dx}\right) dx = \int \frac{1}{EI_{zz}} M_o \, dx = \frac{M_o}{EI_{zz}} \int dx,$$

or

$$\frac{dv(x)}{dx} = \frac{M_o}{EI_{zz}} x + c_1.$$

Integrating again yields an expression for the deflection curve $v(x)$:

$$\int \frac{d}{dx}[v(x)]dx = \int \left(\frac{M_o}{EI_{zz}} x + c_1\right) dx,$$

or

$$v(x) = \frac{M_o}{2EI_{zz}} x^2 + c_1 x + c_2.$$

Applying the boundary conditions for a fixed end, we get

$$\frac{dv}{dx}(x = 0) = 0 \rightarrow 0 = \frac{M_o}{EI_{zz}}(0) + c_1 \rightarrow c_1 = 0,$$
$$v(x = 0) = 0 \rightarrow 0 = \frac{M_o}{2EI_{zz}}(0)^2 + c_1(0) + c_2 \rightarrow c_2 = 0,$$

Therefore, with $I_{zz} = bh^3/12$ for a rectangular cross section, we have

$$v(x) = \frac{6M_o x^2}{Ebh^3},$$

with the deflection at the end (often denoted by δ) where $x = L$, being

$$\delta = v(x = L) = \frac{6M_o L^2}{Ebh^3}.$$

Although this was a simple example, with $M_z = M_o$ and $V = 0$ for all x, it illustrates the general approach, which is our primary goal.

Example 5.9 Find the deflection curve $v(x)$ and the maximum deflection $\delta = v(x = L)$ for the beam in Example 5.7.

Solution: Recalling that the moment $M_z(x) = P(x - L)$, Eq. (5.43) can be integrated once to obtain the slope:

$$EI_{zz}\int \frac{d}{dx}\left(\frac{dv}{dx}\right)dx = \int M_z\,dx = \int P(x - L)dx,$$

or

$$EI_{zz}\frac{dv}{dx} = P\left(\frac{x^2}{2} - xL\right) + c_1.$$

Integrating again, we have

$$EI_{zz}\int \frac{d}{dx}[v(x)]dx = \int \left[P\left(\frac{x^2}{2} - xL\right) + c_1\right]dx$$

$$EI_{zz}v(x) = P\left(\frac{x^3}{6} - \frac{x^2 L}{2}\right) + c_1 x + c_2.$$

Applying the boundary conditions for a fixed end, we get

$$EI_{zz}\frac{dv}{dx}(x = 0) = 0 = P\left(\frac{(0)^2}{2} - (0)L\right) + c_1 \rightarrow c_1 = 0$$

and

$$EI_{zz}v(x = 0) = 0 = P\left(\frac{(0)^3}{6} - \frac{(0)^2 L}{2}\right) + c_1(0) + c_2 \rightarrow c_2 = 0.$$

Thus, the deflection curve for a rectangular cross-section is,

$$v(x) = \frac{P}{EI_{zz}}\left(\frac{x^3}{6} - \frac{x^2 L}{2}\right) = \frac{12P}{Ebh^3}\left(\frac{x^3}{6} - \frac{x^2 L}{2}\right).$$

The maximum deflection is obviously at $x = L$; hence,

$$\delta = v(L) = \frac{12P}{Ebh^3}\left(\frac{L^3}{6} - \frac{L^3}{2}\right) = \frac{-4PL^3}{Ebh^3},$$

or, for any shaped cross section,

$$\delta = -\frac{PL^3}{3EI_{zz}}.$$

Note the minus sign, which indicates that the beam deflects downward given the downward transverse load.

Example 5.10 Find the deflection curve for the beam in Fig. 5.15.

Solution: The free-body diagram for the whole structure reveals that

$$\sum F_x = 0 \rightarrow R_x = 0,$$
$$\sum F_y = 0 \rightarrow R_y - P = 0,$$
$$R_y = P,$$
$$\sum M_z)_A = 0 \rightarrow -M_w + M_o - PL = 0,$$
$$M_w = M_o - PL.$$

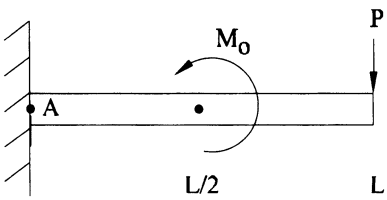

FIGURE 5.15 A cantilevered beam with a concentrated moment applied in the middle and a concentrated transverse load at the end. Because of these concentrated loads, two cuts are necessary for analysis.

Similarly, a free-body diagram of the segment from $0 \le x < L/2$ reveals that

$$\sum F_x = 0 \rightarrow f = 0,$$
$$\sum F_y = 0 \rightarrow P - V(x) = 0,$$
$$V(x) = P \quad \text{for} \quad 0 \le x < \frac{L}{2},$$
$$\sum M_z)_A = 0 \rightarrow M_z - Vx - M_o + PL = 0,$$
$$M_z = P(x - L) + M_o \quad \text{for} \quad 0 \le x < \frac{L}{2},$$

whereas a free-body diagram for the segment from $L/2 < x \le L$ reveals that

$$\sum F_x = 0 \rightarrow f = 0,$$
$$\sum F_y = 0 \rightarrow P - V(x) = 0,$$
$$V(x) = P \quad \text{for} \quad \frac{L}{2} < x \le L,$$
$$\sum M_z)_A = 0 \rightarrow M_z + M_o - Vx - M_o + PL = 0,$$
$$M_z(x) = P(x - L) \quad \text{for} \quad \frac{L}{2} < x \le L,$$

Now, to find the deflections, we appeal to the moment-curvature relation

$$EI_{zz}\frac{d^2v}{dx^2} = M_z(x),$$

but because of the discontinuity at $x = L/2$, the moment-curvature relation should be considered via two equations. Hence,

(1) $EI_{zz}\dfrac{d^2v_1}{dx^2} = P(x - L) + M_o \quad 0 \le x \le \dfrac{L}{2},$

(2) $EI_{zz}\dfrac{d^2v_2}{dx^2} = P(x - L), \quad \dfrac{L}{2} \le x \le L.$

For (1), we integrate two times and denote the associated deflection curve as v_1, namely

$$EI_{zz}\int \frac{d}{dx}\left(\frac{dv_1}{dx}\right)dx = \int [P(x-L)+M_o]\,dx,$$

$$EI_{zz}\frac{dv_1(x)}{dx} = P\left(\frac{1}{2}x^2 - Lx\right) + M_o x + c_1,$$

$$EI_{zz}\int \frac{d}{dx}[v_1(x)]dx = \int \left[P\left(\frac{1}{2}x^2 - Lx\right) + M_o x + c_1\right]dx,$$

$$EI_{zz}v_1(x) = P\left(\frac{1}{6}x^3 - \frac{L}{2}x^2\right) + \frac{M_o}{2}x^2 + c_1 x + c_2.$$

For (2), we likewise integrate two times and denote the associated deflection curve as v_2:

$$EI_{zz}\int \frac{d}{dx}\left(\frac{dv_2}{dx}\right)dx = \int P(x-L)\,dx,$$

$$EI_{zz}\frac{dv_2(x)}{dx} = P\left(\frac{1}{2}x^2 - Lx\right) + c_3,$$

$$EI_{zz}\int \frac{d}{dx}[v_2(x)]dx = \int \left[P\left(\frac{1}{2}x^2 - Lx\right) + c_3\right]dx,$$

$$EI_{zz}v_2(x) = P\left(\frac{1}{6}x^3 - \frac{L}{2}x^2\right) + c_3 x + c_4.$$

Applying the boundary conditions for a fixed end,

$$\frac{dv_1}{dx}(x=0) = 0 \rightarrow c_1 = 0,$$
$$v_1(x=0) = 0 \rightarrow c_2 = 0,$$

we thus have

$$v_1(x) = \frac{1}{EI_{zz}}\left[P\left(\frac{1}{6}x^3 - \frac{L}{2}x^2\right) + \frac{M_o}{2}x^2\right] \quad \left(\text{for } 0 \le x < \frac{L}{2}\right).$$

Two more boundary conditions are needed to find c_3 and c_4. Unfortunately, the boundary conditions for a free end do not provide anything useful. Hence, let us look for other conditions, like continuity of slope and deflection at $x = L/2$; that is, the two solutions should match at $x = L/2$. For example,

$$\frac{dv_1(L/2)}{dx} = \frac{dv_2(L/2)}{dx} \rightarrow$$
$$\frac{1}{EI_{zz}}\left\{P\left[\frac{(L/2)^2}{2} - L\left(\frac{L}{2}\right)\right] + M_o\left(\frac{L}{2}\right)\right\} = \frac{1}{EI_{zz}}\left[P\left(\frac{(L/2)^2}{2} - L\left(\frac{L}{2}\right)\right) + c_3\right].$$

Simplifying, we have

$$c_3 = M_o\left(\frac{L}{2}\right).$$

Similarly, at $x = L/2$, $v_1(L/2) = v_2(L/2)$, and therefore

$$\frac{1}{EI_{zz}}\left[P\left(\frac{(L/2)^3}{6} - \frac{L(L/2)^2}{2}\right) + \frac{M_o}{2}\left(\frac{L}{2}\right)^2\right]$$
$$\frac{1}{EI_{zz}}\left[P\left(\frac{(L/2)^3}{6} - \frac{L(L/2)^2}{2}\right) + M_o\left(\frac{L}{2}\right)^2 + c_4\right],$$

or

$$\frac{M_oL^2}{8} = \frac{M_oL^2}{4} + c_4 \rightarrow c_4 = M_oL^2\left(\frac{1}{8} - \frac{1}{4}\right) = -\frac{M_oL^2}{8}.$$

Therefore,

$$v_2(x) = \frac{1}{EI_{zz}}\left[P\left(\frac{x^3}{6} - \frac{Lx^3}{2}\right) + \frac{M_oL}{2}x - \frac{M_oL^2}{8}\right] \quad \left(\text{for } \frac{L}{2} \le x \le L.\right).$$

Finally, we are interested in $v(x = L/2) = \delta_c$ and $v(x = L) = \delta_b$. Using the second solution, which is good for $L/2 \le x \le L$,

$$\delta_c = \frac{1}{EI_{zz}}\left[P\left(\frac{(L/2)^3}{6} - \frac{L(L/2)^2}{2}\right) + \frac{M_oL}{2}\left(\frac{L}{2}\right) - \frac{M_oL^2}{8}\right] = -\frac{5PL^3}{48EI_{zz}} + \frac{M_oL^2}{8EI_{zz}}$$

and

$$\delta_b = \frac{1}{EI_{zz}}\left[P\left(\frac{L^3}{6} - \frac{L^3}{2}\right) + \frac{M_oL^2}{2} - \frac{M_oL^2}{8}\right] = -\frac{PL^3}{3EI_{zz}} + \frac{3M_oL^2}{8EI_{zz}}.$$

Note: If $M_o = 0$, then the end deflection δ_b is the same as that calculated in Example 5.9 as expected.

Finally, as a check, note that we can also use the solution for $v_1(x)$ to find δ_c:

$$\delta_c = \frac{1}{EI_{zz}}\left\{P\left[\frac{1}{6}\left(\frac{L}{2}\right)^3 - \frac{L}{2}\left(\frac{L}{2}\right)^2\right] + \frac{M_o}{2}\left(\frac{L}{2}\right)^2\right\} = -\frac{5PL^3}{48EI_{zz}} + \frac{M_oL^2}{8EI_{zz}}$$

which matches that from $v_2(x)$, as it should.

5.4 Transducer Design: The AFM

5.4.1 Introduction

Recall from Chap. 1 that biomechanics emerged as a distinct field of study in the mid-1960s due, in large part, to parallel advances in both theory (e.g., continuum mechanics and numerical methods) and technology (e.g., computers). Indeed, scientific advances often result from the development of either a new *enabling technology* or a clever application of existing technology in a new way (e.g., X-ray crystallography aided in the discovery of the basic structure of DNA).

The history of biology reveals, for example, the important role of microscopy in our continuing understanding of the structure and behavior of living things. It was via a primitive two-lens light microscope that Robert Hooke (1635–1703) first observed remnant walls in cork, which led him to introduce the term cell, a word coming from the Latin meaning "little room." Likewise, it was through the use of a light microscope that Malpighi (1628–1694) first observed capillaries in lung tissue, which provided evidence for Harvey's (1578–1657) bold idea of "porosities in the flesh" that allowed blood to flow from arteries to veins. Using the light microscope, Schleiden (1804–1881) and Schwann (1810–1882) suggested that cells are the fundamental unit of life. Indeed, throughout the history of biology, one finds the important role of microscopy (e.g., see Harris 1999; Lodish et al. 2000).

Although by the word "microscopy" we typically think of an optical instrument that increases, via a series of lenses, the apparent size of an object, there are now a host of technologies available: the scanning electron microscope, transmission electron microscope, confocal microscope, and two-photon microscope to name a few. The advantage of having multiple technologies is that one can exploit their particular advantages as needed. For example, the light microscope (LM) can resolve only on the order of 0.2 μm or (200 nm), but the transmission electron microscope (TEM) has a resolution of 0.1 nm. The latter allows one to probe subcellular components as needed in cell mechanics. Whereas the LM and TEM provide information within cross sections, the

scanning electron microscope (SEM) provides information on the 3-D surface structure to a resolution of 10 nm. For more information on these and related microscopic techniques, see Lodish et al. (2000). Here, however, let us consider a recent technology having a particular utility in biomechanics.

5.4.2 The Atomic Force Microscope

First reported in 1986, the atomic force microscope (AFM) has become a widely used tool in the study of protein and cell structure and properties (Binnig et al. 1986; Radmacher et al. 1992). Briefly, the AFM is similar in concept to a profilometer, a device that measures surface contours on hard materials via a moving stylus. As shown in Fig. 5.16, the AFM consists of three primary components: a flexible cantilever beam with a rigid end tip that can be dragged across the surface of a soft sample or used to indent the sample; an optical lever, consisting of a precision laser and photodetector that can measure changes in the angle of the laser light that are associated with the deflection of the cantilever; and a precision piezoelectric *x*-*y*-*z* stage that can either move the cantilever beam or move the sample relative to a fixed beam. The cantilever beams are very small, typically 100–400 μm in length with a tip having a 10–50-nm radius of curvature; they are made using silicon-based nanofabrication techniques. The structural stiffness of the beam is usually quoted as a "spring constant," often on the order of 0.004–1.85 N/m. It is because of this small stiffness that the AFM can resolve forces exerted by atoms, as, for example, van der Waals forces, Coulomb interactions, and hydration forces. The AFM is typically used in one of a few different modes. In the constant-force mode, the cantilever tip is dragged across the surface of a sample while the *x*-*y*-*z*

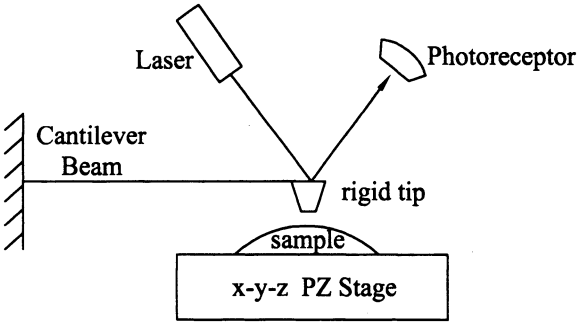

FIGURE 5.16 Schema of the basic components of an atomic force microscope (AFM). The deflection of the cantilevered beam (i.e., probe) is measured with an optical lever consisting of a laser source and photoreceptor (cf. Fig. 4.21). The sample is placed on a piezoelectric (PZ) stage that can move in *x*-*y*-*z*. In some systems, the PZ stage moves the probe rather than the sample, but the net effect is the same.

piezoelectric stage moves the sample (or cantilever) so as to keep the tip-to-sample contact force constant. By tracking the x-y-z changes in position, one can construct a topological map of the surface of the sample. In this mode, one can resolve positions on the order of nanometers (nm). In the indentation mode, the tip can be used to indent the surface of the sample, with measured indentation force–depth data providing information on the local mechanical properties of the sample. In this case, indentation depths are usually on the order of 50–500 nm, often in cells that are less than 2 μm thick. Costa and Yin (1999) showed, therefore, that the associated sample strains are not small and thus one often should not use a linearized analysis (although most do) to infer the mechanical properties of cells using the AFM. Indeed, the associated boundary value problem is very complex and is not discussed here. Rather, we simply note that because the AFM is based on a cantilevered beam subjected to bending, we can examine the design of the device using the methods found in Sects. 5.2 and 5.3.

5.4.3 *Illustrative Example*

Let us assume that an AFM device is constructed of a cantilevered LEHI beam of length L, with Young's modulus E, and a second moment of area $I_{zz} = I$. Moreover, let us assume that the end deflection $\delta \equiv v$ at $x = L$ is inferred from a measure of the end slope $\phi = dv/dx$ at $x = L$, as determined by the laser. If the end load P is directed upward and is transverse to the beam, we note that (cf. Example 5.9)

$$EI_{zz}\frac{d^2v}{dx^2} = M_z(x) = P(L - x),$$

from which upon two integrations and evaluation of boundary conditions ($v(x = 0) = 0$ and $dv(x = 0)/dx = 0$), we have

$$v(x) = \frac{Px^2}{6EI}(3L - x) \rightarrow v(x = L) \equiv \delta = \frac{PL^3}{3EI},$$

or

$$P = \left(\frac{3EI}{L^3}\right)\delta \rightarrow P = k\delta,$$

where k is an effective stiffness for the device having units of force per length; given its analogy with a spring wherein $f = kx$, the k in $P = k\delta$ is called the AFM spring constant. Question: If $L = 400$ μm and the beam is made of silicon ($E \sim 166$ GPa), what value of I would yield a typical value of $k = 1.0$ N/m.

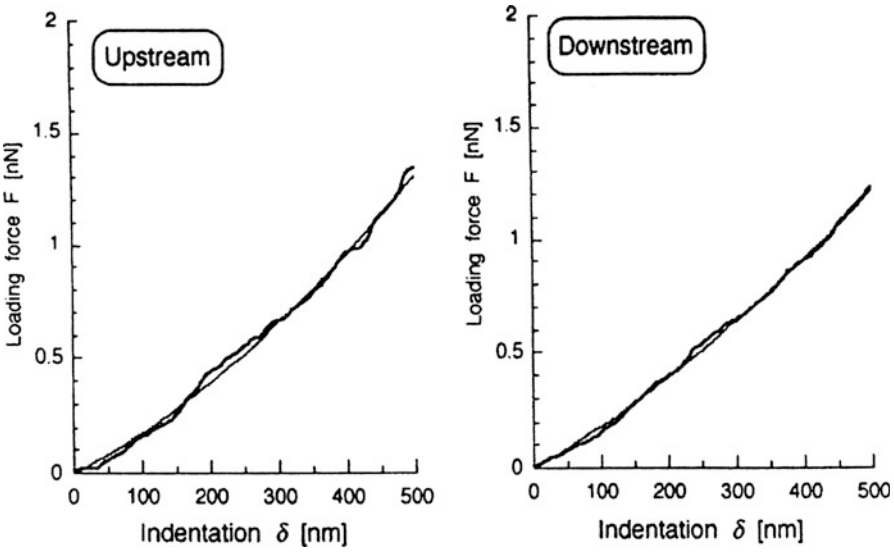

FIGURE 5.17 Measurement of the mechanical response of an isolated endothelial cell to an AFM indentation force. Shown are the force–indentation data, which reveal a nonlinear character and that the upstream portion of the cell tends to be slightly stiffer than the downstream portion when subjected to a flow-induced shear stress. [From Sato et al. (2000) J Biomech 33:127–135, with permission from Elsevier].

Moreover, if the beam is rectangular in cross section with a width $b = 5h$, where h is the height, and $I = bh^3/12$, what is the required thickness of the cantilever? Clearly, these and similar questions can be answered (do it) using ideas discussed herein.

In summary, the AFM has become a widely used device to study both the geometry and properties of living cells (e.g., see Figs. 5.17 and 5.18). Although some inappropriately interpret cell properties using a linearized analysis, we see that our linearized beam theory can again be used in the design of the device itself. We must always remember, therefore, under what conditions derived relations apply.

Observation 5.2. Mathematical solutions to problems of beam bending have far reaching implications in biomechanics and biophysics, but here we consider one particular example. Adherent cells, including those that form monolayers on surfaces as well as those found within the extracellular matrix, often interact with their surroundings via specialized transmembrane structures called integrins. Recall from Sect. 1.4 that integrins consist of heterodimeric glycoproteins denoted as α and β units. Although integrin based cell–matrix interactions need to be weak to allow a cell to realign or migrate, they need to be strong

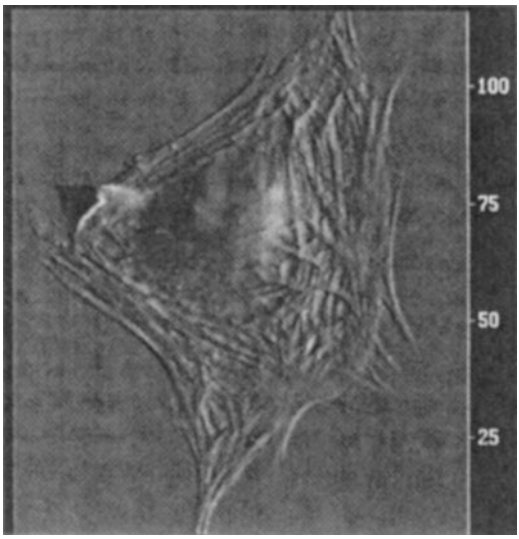

FIGURE 5.18 In the so-called constant-force mode, the AFM can measure the surface topography. Shown here is a single cell, with the region of the nucleus very clear. Such cells tend to adopt very different shapes in vivo wherein they are embedded in a 3-D plexus of extracellular matrix material and have extensive cell-to-cell junctions. There is much that we can learn from tests on isolated cells, and similarly from tests on cell cultures, yet we must remember that it is because of their extreme sensitivity to changes in applied loads (which we seek to measure) that their response in an artificial environment will be different from that in vivo. (Courtesy of Dr. G. Meininger, University of Missouri Dalton Cardiovascular Research Center).

to enable the cell to fashion or remodel the matrix. Strengthening of cell–matrix interactions can be achieved by clustering integrins into increasingly larger groups ranging from *nascent adhesions* to *focal contacts* (~1 μm in diameter), *focal adhesions* (~6 μm in diameter), and ultimately *super focal adhesions* (10–30 μm in diameter). See Hinz (2010) for a detailed discussion in terms of the biomechanics of myofibroblasts.

Of particular interest is how much force a cell can exert on the extracellular matrix via any of these clusters of integrins. Recalling the solution for the end deflection δ of an initially straight cantilevered beam, namely $\delta = PL/3EI$ (see Example 5.9), a number of groups have constructed experimental platforms consisting of arrays of micro-cantilevered beams (like a "bed of nails") that can be functionalized on the ends (e.g., with fibronectin). Cells can then be placed on the platform and contracted via exposure to an agonist. Thus, by monitoring the end deflection of each cantilever and knowing the Young's modulus and geometry, one can infer the transverse end loads ($P = 3EI\delta/L$) exerted by the

cell on its surroundings. Again, therefore, theory can help one both to design and interpret novel experiments.

Finally, note two interesting observations regarding this experiment. First, because a cell must respect equilibrium, the forces must sum (vectorially) to zero if the cell is not migrating (i.e., accelerating), which provides an internal consistency check on the measurements. Second, it has been observed that, in general, cell generated forces scale linearly with integrin cluster area, which suggests that cells seek to maintain constant the stress (force per area) at these clusters, typically around 3–5 kPa. This finding supports further the fundamental concept of *mechanical homeostasis* in mechanobiology (cf. Humphrey (2008) as well as Sect. 11.1).

Example 5.11 Find restrictions on the mechanical resolution of a typical immersed AFM probe due to thermal noise that arises due to the collision of water molecules with the probe.

Solution: As noted by Ethier and Simmons (2007), an immersed probe on an atomic force microscope (AFM) will be subject to random collisions by water molecules undergoing thermal motion. The average energy per molecule at temperature T (e.g., 310 K, or 37 °C) is given by $\frac{1}{2}k_BT$, where $k_B = 1.3807 \text{ x } 10^{-23}$ J/K is the Boltzmann constant. As we saw in the prior section, the mechanical force on the AFM probe due to a transverse end deflection δ is $P = k\delta$, where k is an effective bending stiffness. Hence, the mechanical energy stored due to deflection is $\frac{1}{2}k\delta^2$. If we assume that thermally induced collisions between water molecules and the probe cause a deflection δ, then $\frac{1}{2}k_BT = \frac{1}{2}k\delta^2$, or $\delta^2 = (k_B/k)T$. The associated thermally induced force on the probe is thus $P = \sqrt{(kk_BT)}$. If $k = 0.05$ N/m at 310 K, then $P \sim 1.46 \text{ x } 10^{-11}$ N or $P \sim 14.6$ pN, which would limit the resolution of the device.

5.5 Principle of Superposition

Simply put, this principle asserts that, under certain conditions, one may add the solutions of multiple "simpler" problems to obtain the solution of a more complex problem. Superposition is particularly useful, therefore, when a complex problem can be analyzed in terms of simpler solutions which are well known, such as, the stresses due to extension/compression of an axial rod and the inflation of a thin-walled cylindrical tube (cf. Example 3.3). Indeed, we have already used this principle in many different ways, including the use of the flexure formula for problems involving shear due to transverse loads.

Here, therefore, we wish to emphasize further that it is very important to know when this principle applies and when it does not. Whereas universal solutions can be superimposed, for they are valid for all materials and levels of strain, it is also important to recognize that solutions to linear problems can also be superimposed. The latter should be familiar to those who have had a course in ordinary differential equations wherein we often exploit superposition; the so-called *homogenous* and *particular* solutions can be added when the differential equation is linear.

In this section, therefore, let us explore the utility of the principle of superposition in beam problems wherein the governing differential equations for the deflection are linear [cf. Eqs. (5.43) and (5.46)]; by linear, of course, we mean linear in the deflection $v(x)$, note that the right-hand side of the equation is linear in x. In particular, we shall see that this approach is very useful in two different classes of problem. Let us now illustrate this utility via two examples.

Example 5.12 Find the deflection curve $v(x)$ for a cantilevered beam subjected to a linearly increasing distributed load $q(x)$ and an applied moment M_o at the end. Assume that the beam exhibits a LEHI behavior, is of length L, is initially straight, and has a constant rectangular cross section.

Solution: Let us divide this "complex" problem into two simpler problems: a cantilever subjected to a uniformly increasing load $q(x)$ and an identical cantilever subjected to an end moment M_o. For "beam 1," our governing differential equation is

$$EI_{zz}\frac{d^4v_1}{dx^4} = -q(x) = -q_o\left(\frac{x}{L}\right),$$

where q_o is the value of $q(x)$ at the end. Integrating this equation four times yields

$$EI_{zz}\frac{d^3v_1}{dx^3} = -\frac{q_o}{L}\left(\frac{x^2}{2}\right) + c_1,$$

$$EI_{zz}\frac{d^2v_1}{dx^2} = -\frac{q_o}{L}\left(\frac{x^3}{6}\right) + c_1x + c_2,$$

$$EI_{zz}\frac{dv_1}{dx} = -\frac{q_o}{L}\left(\frac{x^4}{24}\right) + c_1\left(\frac{x^2}{2}\right) + c_2x + c_3,$$

$$EI_{zz}v_1(x) = -\frac{q_o}{L}\left(\frac{x^5}{120}\right) + c_1\left(\frac{x^3}{6}\right) + c_2\left(\frac{x^2}{2}\right) + c_3x + c_4$$

for which we need four boundary conditions:

(a) $v_1(x=0)=0$,

(b) $\dfrac{dv_1}{dx}(x=0)=0$,

(c) $M_z(x=L)=0=EI_{zz}\dfrac{d^2v_1(x=L)}{dx^2}$,

(d) $V(x=L)=0=EI_{zz}\dfrac{d^3v_1(x=L)}{dx^3}$.

Hence, from (a), we have $c_4=0$, and from (b), we have $c_3=0$. Similarly, from (d), we have $c_1=q_oL/2$, and thus from (c), we have $c_2=-q_oL^2/3$. Our first solution is

$$EI_{zz}v_1(x)=-\frac{q_o}{L}\left(\frac{x^5}{120}\right)+\frac{q_oL}{2}\left(\frac{x^3}{6}\right)-\frac{q_oL^2}{3}\left(\frac{x^2}{2}\right),$$

or

$$v_1(x)=\frac{1}{EI_{zz}}\left(\frac{-q_o}{120L}\right)\left(x^5-10L^2x^3+20L^3x^2\right).$$

Next, for "beam 2," we have

$$EI_{zz}\frac{d^2v_2}{dx^2}=M_o,$$

which can be integrated twice to yield

$$EI_{zz}\frac{dv_2}{dx}=M_ox+c_5,$$
$$EI_{zz}v_2(x)=M_o\left(\frac{x^2}{2}\right)+c_5x+c_6,$$

for which we need but two boundary conditions:

(e) $v_2(x=0)=0$,

(f) $\dfrac{dv_2(x=0)}{dx}=0$.

Hence, $c_5=0$ and $c_6=0$ and

$$v_2(x)=\frac{1}{2EI_{zz}}\left(M_ox^2\right).$$

The solution for our original problem is thus

$$v(x) = v_1(x) + v_2(x)$$

by superposition.

Clearly, we could obtain solutions to even more complicated problems by simply adding together the solutions of multiple (appropriate) simpler problems. Here, however, let us consider the second primary utility of the principle of superposition in problems of beam bending. Recall that a statically indeterminate problem is one that cannot be solved via statics alone. In traditional problems of beam bending, we recall further that we have but three general equilibrium equations ($\Sigma F_x = 0$, $\Sigma F_y = 0$, $\Sigma M_Z = 0$) to find the reactions. Hence, in cases in which there are four or more reactions (i.e., a statically indeterminate problem), we must seek additional equations to solve the problem. Let us illustrate how the principle of superposition can be useful in this regard.

Example 5.13 Find the reactions for the beam in Fig. 5.19 assuming that L, E, I_{zz} and q_o are all known.

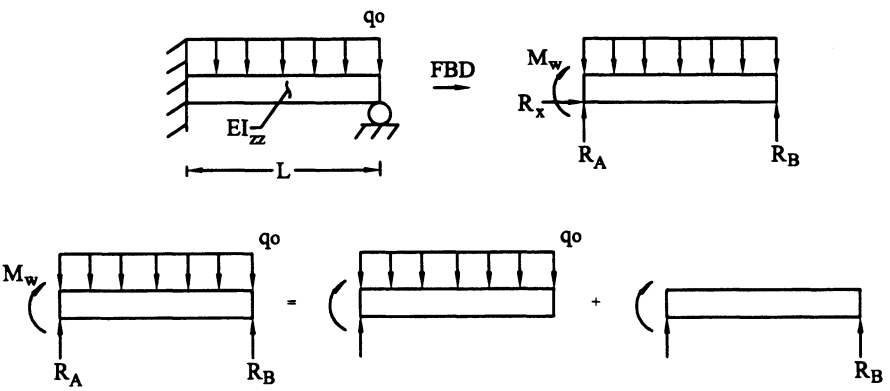

FIGURE 5.19 Statically indeterminate beam, cantilevered on one end and supported by a roller on the other. The three equations of static equilibrium are thus insufficient to determine the four reactions: M_w, R_A, R_B, and R_x at A; that is, whereas R_x can be shown to be zero via axial force balance, the remaining equations (vertical force balance and moment balance) are not sufficient to find the remaining three unknowns. Also shown are free-body diagrams of two convenient subproblems: a cantilevered beam subjected to a uniformly distributed load and a cantilevered beam subjected to a transverse end load. In the latter case, we can treat the reaction R_B as we would an applied load and thus solve the problem as usual.

Solution: First, note that equilibrium of the whole requires that

$$\sum F_x = 0 \rightarrow R_x = 0,$$
$$\sum F_y = 0 \rightarrow R_A + R_B - \int_0^L q_o dx = 0,$$
$$\sum M_z)_A = 0 \rightarrow R_B L - \int_0^L (q_o x) dx - M_w = 0,$$

which yields three equations in terms of four unknowns (R_x, R_A, R_B, M_w). To generate a fourth equation, let us divide the problem into two problems (Fig. 5.19): a cantilever subjected to a uniformly distributed load q_o and a cantilever subjected to an end load R_B (whose value is as yet unknown). Clearly, we know the solutions for the deflection curves for each of these "simpler" problems. From an analysis similar to that in the previous example, show that

$$EI_{zz} v_1(x) = -q_o \left(\frac{x^4}{24}\right) + q_o L \left(\frac{x^3}{6}\right) - \frac{q_o L^2}{2} \left(\frac{x^2}{2}\right),$$

whereas from Example 5.9 (with $P = -R_B$), we have

$$EI_{zz} v_2(x) = -R_B \left(\frac{x^3}{6}\right) + R_B L \left(\frac{x^2}{2}\right).$$

Note: The direction of R_B is opposite the previously considered end load P, but otherwise the present problem is no different than that considered earlier. Hence, the solution to our original problem is

$$v(x) = v_1(x) + v_2(x),$$

subject to the constraint that

$$v_1(x = L) + v_2(x = L) = 0$$

because the roller at $x = L$ does not allow a deflection [i.e., $v(x = L) = 0$ is a boundary condition for the full problem]. This constraint provides an additional equation in terms of one of the original four unknowns; thus, we have succeeded in identifying four equations (three from equilibrium and one from a kinematic constraint condition) for our four unknowns and the problem can be solved. In particular, from the constraint condition, we find that

$$0 = -q_o\left(\frac{L^4}{24}\right) + q_oL\left(\frac{L^3}{6}\right) - \frac{q_oL^2}{2}\left(\frac{L^2}{2}\right) + (-R_B)\left(\frac{L^3}{6}\right) + R_BL\left(\frac{L^2}{2}\right),$$

$$0 = q_oL^4\left(-\frac{1}{24} + \frac{1}{6} - \frac{1}{4}\right) + R_BL^3\left(-\frac{1}{6} + \frac{1}{2}\right),$$

or

$$R_B = \frac{3}{8}q_oL,$$

hence finding the reaction at B in terms of the known values of q_o and L. Returning to the three equilibrium equations, we can now find R_A and M_w, which, in turn, will allow a full stress analysis. This is left for the reader to complete.

In closing, we emphasize yet again that mechanics is not a subject consisting of solutions to individual problems; rather, it is a subject in which a common method is used to solve diverse problems. Note, therefore, that we have used kinematic constraint conditions earlier to render a problem well posed: in Sect. 4.1.3, we used the condition that the end deflection δ was the same for the bone and the metal prosthesis in an axial load problem, and in Sect. 4.4.2, we used the condition that an angle of twist Θ was likewise the same in a bone–prosthesis torsion problem. *Kinematic constraints*, in the present case matching the deflections from two solutions at a single point in a beam, are thus very useful to impose in many problems and should be considered in problems wherein statics alone does not yield a sufficient number of equations.

Observation 5.3. We have noted that materials and structures can fail via a variety of mechanisms. They can deform excessively and thus cease to fulfill the intended function; they may yield and thus experience a permanent set which prevents them from returning to an original shape or location when unloaded; or they can fracture (i.e., rupture) and thus fail catastrophically. In each of these cases, failure may occur the first time that the applied loads exceed safe values (e.g., the yield stress). Another type of failure that is potentially problematic in many biomechanical problems is *fatigue failure*. In material science, the term "fatigue" denotes a loss in strength of a material due to repeated loading. Fatigue often occurs in three stages: the initiation of small cracks, the propagation of these cracks, and, finally, fracture due to the development of large cracks. A common method to test a material's resistance to fatigue is the "rotating cantilever test." In this test, a cylindrical specimen is

loaded, via a bearing, by a transverse load at its end while the specimen is rotated many (sometimes millions) times. Because the specimen experiences tension on the top and compression on the bottom, material away from the neutral axis experiences a sinusoidal cycle from maximum to minimum tensile and compressive stresses. Tests are performed to failure, with the number of cycles to failure noted. Similar tests at multiple levels of applied load (i.e., maximum stress) reveal differences in the number of cycles to failure at different stresses. When the number of cycles to failure (abscissa) is plotted against the stress during the test (ordinate), one obtains a so-called *S–N* (or stress-number) curve. As one might expect, the number of cycles to failure is greater for lower values of applied stress and, conversely, it is lower for higher values of stress. Given that prosthetic hips and knees must survive millions of cycles due to daily walking or running and, likewise, artificial heart valves must survive over 30 million cycles per year, fatigue failure is an important concern in the biomechanical design of prosthetic devices. Question: Why is fatigue failure less of an issue for biological tissues? Answer: Tissues are continually replaced via a balanced synthesis and degradation of material; hence, the "same" material does not experience the thousands to millions of cycles needed to cause fatigue failure. Of course, repeated surgical replacement of prosthetic devices to renew the material is not a viable option for the biomedical engineer; thus, there is a need to decrease the likelihood of fatigue failure.

Let us note a few additional terms: The *fatigue life* tells us how long a particular component is expected to survive at a particular stress under normal conditions and the *fatigue strength* is the maximum stress for which failure will not occur for a prescribed number of cycles (e.g., 300 million). Fatigue testing is obviously a very important and yet potentially time-consuming activity. For this reason, one often seeks to perform accelerated tests whereby the requisite number of cycles can be achieved in much less time than would be required at the physiological rate. For a heart valve, for example, a 10-year equivalent fatigue test can be performed in 1 year if the tests are performed at 10 Hz rather than the physiological ~1 Hz. Yet, 1 year is still a long time to wait for experimental results and one might be tempted to perform the test at 100 Hz and thus obtain results in ~5 weeks instead of 1 year. One must ask, however, whether the behavior of the material of interest is sensitive to the rate of deformation, because this could adversely affect the results. We shall see in Chap. 11, for example, that strain-rate sensitivity is one of the characteristics of a viscoelastic behavior.

For many polymers, one can alternatively use a concept of time–temperature equivalency (Ferry 1980), which states that similar behaviors occur much faster at higher temperature. Thus, by performing tests at temperatures above service conditions (e.g., at 70 °C rather than 37 °C), one can collect data over much shorter periods. Temperature can have very different effects on other materials, however, including tissue; thus, one must be very careful when employing this

equivalency for experimental expediency. Fatigue testing is nevertheless often time-consuming. Because of its importance, including Food and Drug Administration (FDA) specifications in many cases, the biomechanical engineer must investigate this deeply. We refer the interested reader to books on material science.

5.6 Column Buckling

Recall from Sect. 5.1 that a column is any structural member having one dimension greater than the other two and subjected to a compressive axial load. In some cases, the column may fail due to an excessive load simply by fracture, plastic deformation, or excessive compression. In other cases, however, the primary concern may be the possibility that the column may become unstable and buckle. A simple example of such buckling can be appreciated by taking a plastic ruler and compressing it along its long axis—the sudden bending out, or *buckling*, occurs when a critical value of the compressive load P_{cr} is achieved (Fig. 5.20). Let us now consider the general concept of stability as well as the specific example of column buckling.

5.6.1 Concept of Stability

Consider the two structural members in Fig. 5.21. In each case, statics tells us that the reaction force at the pin is $R_y = W$, the weight of the member. Indeed, in each case, the pin is exerting an upward directed force and we might say that the

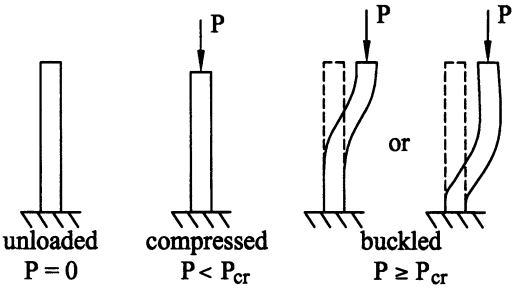

FIGURE 5.20 A cantilevered beam is subjected to a compressive end load P. Initially the beam-column will simply compress and the stress $\sigma_{xx} = -P/A$, as in Chap. 3. After a critical value P_{cr} is reached, the beam column will buckle (i.e., bend abruptly) and the analysis of stress and strain becomes much more complex. Hence, rather than computing these complex states of stress or strain, let us focus simply on that value of P_{cr} that induces buckling.

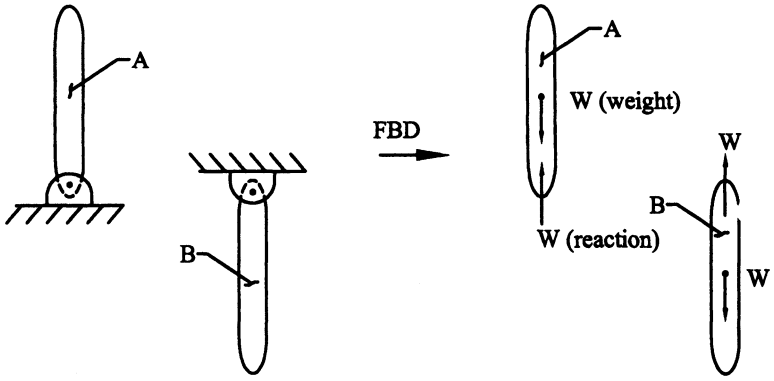

FIGURE 5.21 Illustration of the concept of stability. Although structural members A and B are both in equilibrium, which is to say that the reaction force $R_y = W$ for both, structure A is unstable—a small transverse (i.e., disturbing) load will cause it to swing down and assume a position similar to that of B. Structure B, on the other hand, will simply swing back and forth if disturbed by a small transverse load until it regains its original equilibrium position (assuming air friction or friction in the pin, otherwise with no energy dissipation the member could swing back and forth about the original equilibrium indefinitely).

two problems are statically equivalent. From the perspective of stability, however, these two problems are very different. If we subject member B to a small lateral *disturbing* load, or perturbation, we expect the member to move initially in the direction of the load, but then, like a pendulum, to swing back and forth until it regains its original position (assuming a frictionless pin but resistance to motion due to the air). Conversely, we expect member A to respond very differently to the same lateral disturbing force—we expect it to swing down and eventually gain the position of member B. Note: This experiment is accomplished easily by holding your pen loosely between two fingers in each of the original configurations and subjecting it to a small lateral disturbing force. Although both members A and B are initially in equilibrium, we say that A is unstable and B is stable. *Mechanical stability*, then, is the ability to resist a small disturbing force, which is a very important structural characteristic.

Another good illustration of the concept of stability is seen in Fig. 5.22. In this case, imagine three otherwise identical balls on low friction surfaces. Moreover, imagine the response of each initially centered ball if it is subjected to a small lateral disturbing force. In case A, we easily imagine the ball "rolling off the hill," which is to say, moving in such a way that it cannot regain its original position. We would say that this ball is unstable because the disturbing force caused the ball to find another equilibrium position. Conversely, in case B, we can easily imagine that, provided the disturbing force is not too large, the ball will first move in the direction of perturbation, but then roll back and

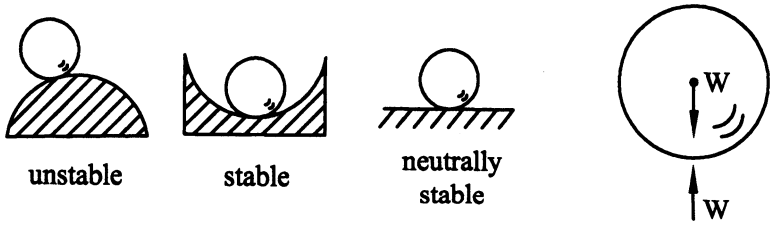

FIGURE 5.22 Another simple illustration of the concept of stability. Although each ball is initially in equilibrium (if centered) and thus has the same initial free-body diagram, a small lateral force will cause the ball on the hill to roll off, whereas a small lateral force will cause the ball in the trough to simply roll back and forth until it comes to rest in its original position (again, assuming some friction in the system). These are called unstable and (asymptotically) stable, respectively. The ball on the flat plate may move only slightly when disturbed; thus, this is called neutrally stable—it need not experience an abrupt change in equilibrium position, but it also need not regain its original position.

forth until it regains its original position. This ball would be said to be (asymptotically) stable. Thus, in cases A and B in Figs. 5.21 and 5.22, we see that mechanical stability is an ability to resist a small disturbing force, which is to say, an ability to regain the original position or configuration following the disturbance. Case C in Fig. 5.22 illustrates one final possibility. In this case, the ball will not regain its original position, but it may not move far from that position. Such cases are called neutrally stable; they are, in fact, a cause for concern, for they may easily degenerate into an instability given slight imperfections (e.g., if the flat surface is at a slight incline). We will consider the static stability of an elastomeric balloon in Chap. 6 and the dynamic stability of an aneurysm in Chap. 11. We should be very mindful, therefore, that stability is an important consideration in biomedical design, analysis, and experimentation with regard to both biomaterials and native tissues. Let us now consider the generic case of column buckling, the classical introduction to stability in engineering mechanics and another subject in mechanics that was touched by the genius of L. Euler.

5.6.2 *Buckling of a Cantilevered Column*

Consider the initially straight but buckled column in Fig. 5.23, which is assumed to exhibit a linear, elastic, homogenous, and isotropic (LEHI) response. If the axial load P is applied through the centroid, we expect one of two possibilities. First, consider the case wherein the column just compresses as an axial rod. In this case, $\sigma_{xx} = -P/A$ (compressive) and the displacement is given by

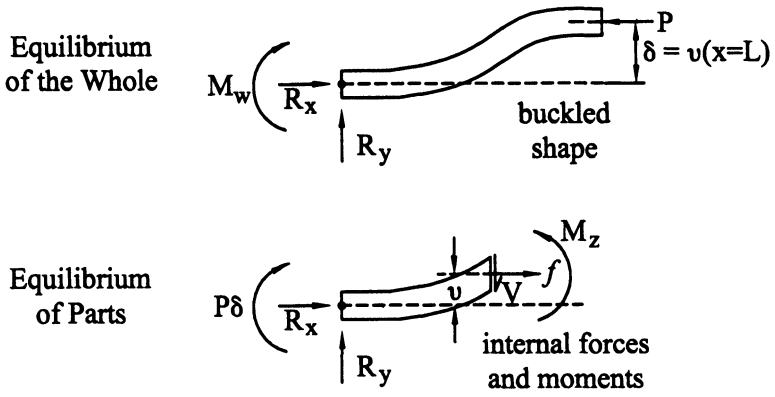

FIGURE 5.23 Detailed free-body diagrams of the whole and part of a cantilevered beam column as shown in Fig. 5.20.

$$u_x(x) - u_x(0) = \int_0^x -\frac{P}{AE}dx = -\frac{P}{AE}x, \tag{5.47}$$

assuming a constant cross section and homogenous constitution. These results are valid as long as $|P| < |P_{cr}|$, the so-called critical buckling load.

If we continued to load the column until $|P| = |P_{cr}|$, however, the situation is very different. As can be seen, the buckled beam appears "bent" and, consequently, as in the prior sections of this chapter, we must consider the bending. The main difference, however, is that it is a compressive load, not a transverse load or applied bending moment, that gives rise to the buckling of the beam. Equilibrium of the whole reveals that the reactions at the wall are (Fig. 5.23)

$$\begin{aligned} \sum F_x = 0 = R_x - P \rightarrow R_x = P, \\ \sum F_y = 0 \rightarrow R_y = 0, \\ \sum M_z)_A = 0 = P\delta - M_w \rightarrow M_w = P\delta, \end{aligned} \tag{5.48}$$

where $v(x = L) = \delta$. Equilibrium of the parts thus reveals (Fig. 5.23) that

$$\begin{aligned} \sum F_x = 0 = P + f \rightarrow f = -P, \\ \sum F_y = 0 \rightarrow V = 0, \\ \sum M_z)_A = 0 =\rightarrow M_z - fv - P\delta = 0, \end{aligned} \tag{5.49}$$

or

$$M_z = fv + P\delta = P\delta - Pv. \tag{5.50}$$

Assuming that the moment-curvature relation [Eq. (5.43)] holds in this case of bending, we have

$$EI_{zz}\frac{d^2v}{dx^2} = P\delta - Pv, \tag{5.51}$$

or

$$\frac{d^2v}{dx^2} + \frac{P}{EI_{zz}}v = \frac{P}{EI_{zz}}\delta. \tag{5.52}$$

We recognize from our study of differential equations (reviewed in Appendix 8 of Chap. 8) that this is a second-order, linear, nonhomogenous differential equation with a constant coefficient (for each value of P). It will prove useful, therefore, to let this coefficient be denoted by $k^2 \equiv P/EI_{zz}$, thus yielding our final governing differential equation

$$\frac{d^2v}{dx^2} + k^2v = k^2\delta. \tag{5.53}$$

Because this is a linear equation, let us first seek its homogenous and then its particular (i.e., nonhomogenous) solutions whereby $v(x) = v_h(x) + v_p(x)$. First, for the homogenous equation, note that it can be written in operator form as

$$\frac{d^2v_h}{dx^2} + k^2v_h = 0 \leftrightarrow \left(D^2 + k^2\right)v_h = 0, \tag{5.54}$$

whereby we have a solution if $D = \pm ki$, where $i = \sqrt{-1}$. We know that the solution of such equations can be assumed to be of the form

$$v_h(x) = e^{(a+bi)x} = e^{ax}(c_1 \cos bx + c_2 \sin bx). \tag{5.55}$$

Hence, for our problem, we have $a = 0$ and $b = k$; thus,

$$v_h(x) = c_1 \cos kx + c_2 \sin kx. \tag{5.56}$$

As an exercise, verify that this solution does in fact satisfy the homogenous differential equation; this is accomplished easily by taking the second derivative and substituting back into Eq. (5.54).

Next, for the particular solution, note that the right-hand side of Eq. (5.53) is constant and thus let

$$v_p(x) = A, \tag{5.57}$$

from which we see that this is a solution of the nonhomogenous equation provided that $A = \delta$. Thus, our full solution is

$$v(x) = c_1 \cos kx + c_2 \sin kx + \delta. \tag{5.58}$$

The boundary conditions are

$$\begin{aligned} &v(x=0) = 0 \rightarrow 0 = c_1 + \delta \rightarrow c_1 = -\delta. \\ &\frac{dv}{dx}(x=0) = 0 \rightarrow 0 = c_2 k \rightarrow c_2 = 0. \end{aligned} \tag{5.59}$$

Hence,

$$v(x) = \delta(1 - \cos kx), \tag{5.60}$$

where $\delta \equiv v(x = L)$ provides the constraint condition that

$$\delta = \delta(1 - \cos kL), \tag{5.61}$$

which, in turn, requires that $\cos kL = 0$ for all k. The cosine function equals zero, of course, at $\pi/2$, $3\pi/2$, $5\pi/2$, ...; hence, we must have

$$KL = n\frac{\pi}{2}, \quad n = 1, 3, 5, ... \tag{5.62}$$

Now, recalling that $k^2 = P/EI_{zz}$, this says that

$$\sqrt{\frac{P}{EI_{zz}}}\, L = \frac{n\pi}{2} \tag{5.63}$$

or that a value (magnitude) of the compressive axial load P for which we have buckling is

$$P = \frac{n^2\pi^2}{4L^2} EI_{zz}. \tag{5.64}$$

We are interested, of course, in the smallest buckling load, called P_{cr} or the *critical buckling load*, which is given by $n = 1$, and therefore

$$P_{cr} = \frac{\pi^2}{4L^2} EI_{zz} \tag{5.65}$$

for this case of a cantilevered column subjected to an axial end load P. Note that the critical buckling load is increased by an increased stiffness of the material E and increased second moment of area I_{zz}. Conversely, P_{cr} is reduced

as the length of the column is increased. All of these effects are intuitive; for example, if we try to buckle a plastic ruler, we can make it more difficult to do so by simply supporting it in such a way that its effective length is reduced. Try it. Likewise, if we increase the stiffness (e.g., use a wooden ruler rather than a plastic one), it is harder to induce buckling, and so too if we increase the cross-sectional area. Indeed, note that the result for P_{cr} depends on I_{zz}. Actually, it is somewhat arbitrary how we define the y and z directions in the cross section, so note that a ruler tends always to buckle in one direction (i.e., in the direction of least thickness), the one associated with the smallest second moment of area.

Finally, a few words about our solution $v(x)$. It may be tempting to draw the buckled shape of the column using our solution for $v(x)$ and k and, indeed, some seek to explain the different buckling modes (shapes) via different values of n (i.e., different curves defined by sines and cosines). One knows, for example, that a buckled plastic ruler could assume various sinusoidal shapes depending on how strongly one pushes on the ends. To try to explain such buckled shapes based on our analysis is ill advised, however, because our solution was based on the moment-curvature relation, which, in turn, was based on the assumption of a small slope ($dv/dx \ll 1$). This assumption is not respected by the buckled shape in general. Hence, we can only use this formulation to find P_{cr}, which is *the load at which buckling is imminent but not realized*. This example serves to remind us again that it is essential to remember and respect all assumptions. To determine the buckled shape, we must first derive and then solve a nonlinear differential equation. This is beyond the present scope.

Finally, note that our governing differential equation (5.52) is not a general equation; it is valid only for a column with a free end. Other boundary conditions will thus modify both the general equation and the associated unknown coefficients in the solution. Each case is solved similarly, but they are different. Consider the following example.

Example 5.14 Find the critical buckling load for the fixed–pinned column in Fig. 5.24.

Solution: First, consider a free-body diagram for the whole structure:

$$\sum F_x = 0 \rightarrow R_x = P,$$

$$\sum F_y = 0 \rightarrow R_y = -N,$$

$$\sum M_z)_o = 0 \rightarrow -M_w + NL = 0,$$

and, thus,

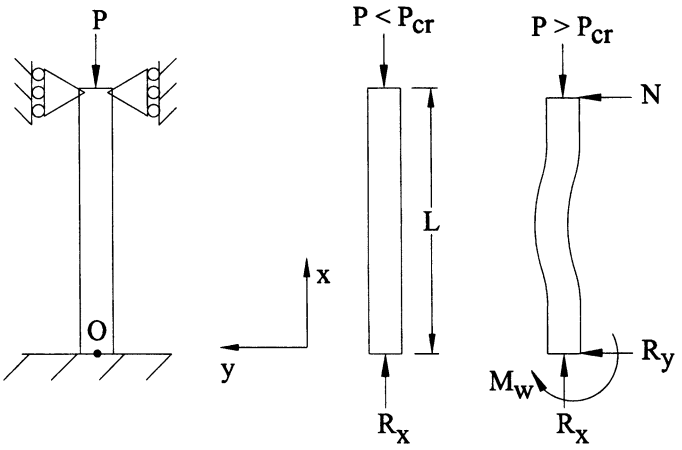

FIGURE 5.24 Solutions of beam-column problems are very sensitive to the boundary conditions. Shown here is a fixed-pinned column.

$$M_w = NL \text{ and } R_y = -\frac{M_w}{L}.$$

Second, consider a free-body diagram for the part (draw it):

$$\sum F_x = 0 \rightarrow f = -P,$$
$$\sum F_y = 0 \rightarrow -\frac{M_w}{L} - V = 0,$$
$$V = -\frac{M_w}{L},$$
$$\sum M_z\big)_o = 0 \rightarrow -M_w + M_z - Vx - v(x)f = 0,$$
$$M_z = M_w - \frac{M_w}{L}x - Pv(x).$$

Thus, from the linearized moment-curvature relation [Eq. (5.43)], we have

$$EI_{zz}\frac{d^2v}{dx^2} = -Pv + M_w\left(1 - \frac{x}{L}\right).$$

Rearranging this relation into standard form, we have

$$\frac{d^2v}{dx^2} + \frac{P}{EI_{zz}}v = \frac{M_w}{EI_{zz}}\left(1 - \frac{x}{L}\right).$$

Consistent with the previous example, the homogeneous solution is

$$v_h(x) = c_1 \cos kx + c_2 \sin kx.$$

For a particular solution, given that the right-hand side is linear in x, assume

$$v_p(x) = c_3 + c_4 x,$$

whereby

$$\frac{dv_p}{dx} = c_4 \text{ and } \frac{d^2 v_p}{dx^2} = 0.$$

Hence, substituting into the governing differential equation for $v_p(x)$

$$0 + \frac{P}{EI_{zz}}(c_3 + c_4 x) = \frac{M_w}{EI_{zz}}\left(1 - \frac{x}{L}\right) \rightarrow c_3 + c_4 x = \frac{M_w}{P} - \frac{M_w}{PL}x$$

and, consequently,

$$c_3 = \frac{M_w}{P} \text{ and } c_4 = -\frac{M_w}{PL}.$$

The full solution then becomes $v(x) = v_h(x) + v_p(x)$, or

$$v(x) = c_1 \cos kx + c_2 \sin kx + \frac{M_w}{P} - \frac{M_w}{PL}x,$$

from which

$$\frac{dv(x)}{dv} = c_1(-k \sin kx) + c_2(k \cos kx) - \frac{M_w}{PL}.$$

Enforcing the boundary conditions at the fixed end, $v(x=0) = 0$ and $dv(x=0)/dx = 0$,

$$0 = c_1 + \frac{M_w}{P} \rightarrow c_1 = -\frac{M_w}{P},$$

$$0 = c_2 k + \frac{M_w}{PL} \rightarrow c_2 = \frac{M_w}{kPL}.$$

Enforcing the boundary conditions at the pinned end, $v(x=L) = 0$,

$$0 = -\frac{M_w}{P}\cos kL + \frac{M_w}{kPL}\sin kL + \frac{M_w}{P} - \frac{M_w}{PL}L,$$

or

$$\frac{1}{kL}\sin kL - \cos kL = 0.$$

Hence,

$$\frac{1}{kL} = \frac{\cos kL}{\sin kL} \rightarrow kL = \tan kL.$$

This is a transcendental (nonlinear) equation, which does not admit a direct solution. However, one can use an iterative numerical method to show that the smallest root is

$$kL \approx 4.4935\,(\text{radians})$$

from which

$$P_{cr} \approx \frac{20.19EI_{zz}}{L^2} = \frac{2.05\pi^2 EI_{zz}}{L^2},$$

the latter of which permits an easier comparison to the previous result.

Chapter Summary

This chapter addresses two of five aforementioned canonical problems in introductory biosolid mechanics: bending of a 1-D structure often referred to as a beam and compressive buckling of a 1-D structure often referred to as a column. The other canonical problems are addressed in Chaps. 3 and 4. Beam bending is considered by many to be amongst the most fundamental problems in solid mechanics, with copious applications in vivo (in the body), ex vivo (outside of the body, but living), and in vitro (literally in glass, but outside of the body in general). Of particular note, knowledge of beam bending is especially useful in the design of both load cells and diverse experiments, with the latter ranging from determination of bending properties of bones (e.g., via a standard 4-point bending test that yields quantities of interest uniform in a central region) to measurement of cellular contraction, focal adhesion strength (e.g., using an array of micro-cantilevered beams), or cell stiffness (e.g., via atomic force microscopy).

As in Chaps. 3 and 4, we sought to find stress in terms of the applied load and geometry and we sought to find strain, or the associated deformation, in terms of

applied load, geometry, and material properties. Equations (5.23) and (5.30) reveal that we accomplished this goal for stress in a standard beam bending problem: the normal stress depends on the local applied load (bending moment M) and geometry (vertical location y and second moment of area I) and similarly the shear stress depends on the local applied load (shear force V) and geometry (location Q, second moment of area I, and thickness b). Nevertheless, as in the case for torsion of a cylindrical structure, the results implicitly depend on a particular constitutive relation (Hooke's law) and thus are not universal. In contrast, Sect. 5.1 revealed that one can determine distributions of the bending moment M and the shear force V from statics alone.

Also as in the case of torsion of a cylindrical structure, we saw that transformation relations are useful in determining principal values of stress in terms of components that are easiest to compute, and that the associated deformations depend on applied load, geometry, and material properties. The latter can be determined via equivalent second, third, or fourth order ordinary differential equations for deflection, the choice of which depends simply on convenience of prescribing the applied load (in terms of moment M, shear V, or uniform load q, respectively). We also saw that the number of necessary *boundary conditions* depended on the order of the differential equation, hence encouraging us to be familiar with the many types of conditions: displacement, rotation, reaction force, and applied moment as revealed in Fig. 5.14. Because of the linearity of these differential equations, we were reminded, just as we learned in our mathematics courses, *that solutions can be superimposed in linear problems*; this property can help simplify finding solutions in some cases.

Finally, this chapter introduced an important area of mechanical analysis, the concept of *stability*. That is, determination of an equilibrium solution does not reveal whether the material or structure can resist small perturbations in loading from equilibrium. Stability (cf. Figs. 5.20, 5.21, and 5.22) is an extremely important issue in theoretical and experimental mechanics, in analysis and design. Although entire courses are devoted to this important topic, we considered only a single problem, the buckling of a column under compressive loading. Again, we introduced a particular constitutive relation (namely, Hooke's law for LEHI behavior) and consequently the results are not universal. Moreover, because of the assumption of small strain and small rotation, this analysis can only determine the critical load at which buckling is imminent, not the post-buckling response. In other words, if post-buckling response is of interest, then one must employ an appropriate nonlinear beam analysis, which is beyond the present scope. Chapters 6 and 11 address simple nonlinear problems that exhibit instabilities.

Appendix 5: Parallel Axis Theorem and Composite Sections

Recall from Appendix 4 of Chap. 4 that the second moment of area I_{zz} is given by

$$I_{zz} = \iint y^2 dy\, dz, \tag{A5.1}$$

where y and z are taken here to be the in-plane coordinates (i.e., cross sectional) and x is directed along the long axis of a beam. Moreover, because of our need to locate the origin of our (o; x, y, z) coordinate system at the centroid [recall Eq. (5.20)], this I_{zz} must likewise be computed relative to the centroid. For simple geometries, such as rectangular or circular, such computations are straightforward, as seen in Appendix 4. In many beam-bending problems, however, the cross section of the beam is often complex, whether it is the cross section of a long bone or the cross section of a beam used as a transducer. For this reason, the so-called *parallel axis theorem* is very useful.

Consider the centroidal coordinate system (y,z) and general cross section shown in Fig. 5.25. Clearly,

$$I_{zz} = \iint y^2 dy\, dz$$

is computed with respect to the centroidal coordinates (y, z), whereas

$$I'_{zz} = \iint (y+d)^2 dA = \iint y^2 dA + 2d \iint y dA + d^2 \iint dA \tag{A5.2}$$

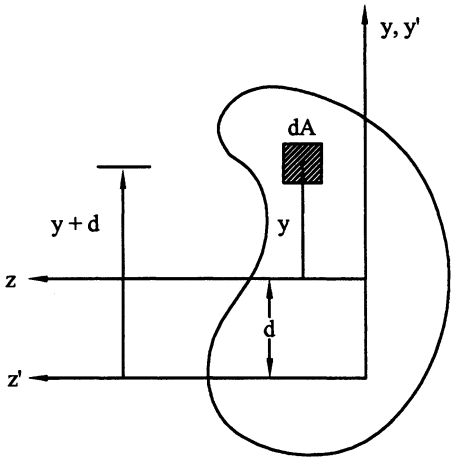

FIGURE 5.25 Coordinate system and generic cross section for deriving the parallel axis theorem; (y, z) are centroidal coordinates, which are very useful in beam theory.

is computed with respect to another coordinate system (y', z') oriented parallel to our centroidal system. In addition to recognizing the second moment of area with respect to the centroidal system, $\iint y^2 dA$, we also recognize the first moment of area $\overline{y}A\iint ydA$, also with respect to the centroidal system (y, z). The value of $\overline{y}$ relative to the centroidal system (i.e., the distance the centroid is from the centroid) is zero, however; thus, we have

$$I'_{zz} = I_{zz} + d^2 A, \tag{A5.3}$$

which is known as the parallel axis theorem. It allows us to compute the second moment of area of a cross section of area A given its "centroidal second moment of area" and the distance d between the centroidal axis z and any parallel axis z' of interest. Clearly, a similar, more general result can be obtained if y and y' do not coincide. Regardless, we emphasize that the parallel axis theorem is very useful for determining the value of the second moment of area of a "composite" cross section relative to the overall centroid. To illustrate this, consider the I-beam cross section shown in Fig. 5.26.

To compute the *overall* centroidal second moment of area, we can use the parallel axis theorem three times to transform the easily computed *individual* centroidal values of rectangles ($bh^3/12$) to the overall centroid; that is, for the top, middle, and bottom parts respectively, we have

$$I_{zz} = \left[\frac{1}{12}bt^3 + \left(\frac{h}{2}+\frac{t}{2}\right)^2 bt\right]_{\text{top}} + \left(\frac{1}{12}th^3 + 0^2 bt\right)_{\text{middle}} + \left[\frac{1}{12}bt^3 + \left(-\frac{h}{2}-\frac{t}{2}\right)^2 bt\right]_{\text{bottom}}, \tag{A5.4}$$

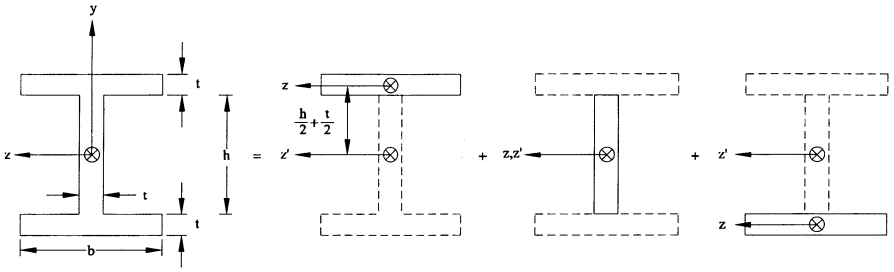

FIGURE 5.26 Illustration that, like first moments of area (cf. Appendix 3 of Chap. 3), second moments of area can be determined using a method of "composite" sections shown by *solid lines*. The parallel axis theorem is fundamental to such determinations.

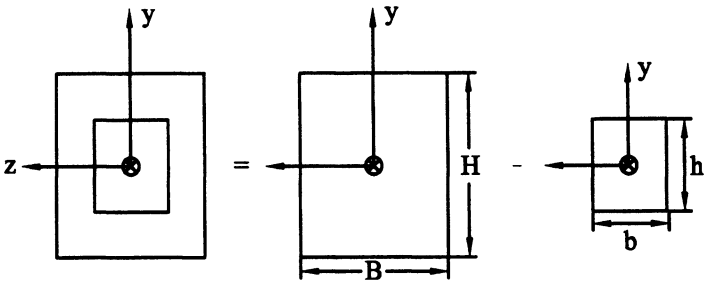

FIGURE 5.27 Another example of the method of composite sections to determine a second moment of area—this time for a cross section with a hole.

which can be simplified algebraically if desired. The two key observations are that the distance squared term d^2A provides a positive contribution regardless of the location of the small part relative to the centroid and that $d = 0$ recovers our standard relation.

Hence, for a composite section

$$I'_{zz}(\text{whole}) = \sum \left(I_{zz} + d^2A\right)_{\text{parts}}, \tag{A5.5}$$

where $(\ldots)_{\text{Parts}}$ is computed relative to the centroidal coordinate system for each part. Note, too, that one can use this idea to compute the second moment of area of a hollow cross section. For example, the simple case in Fig. 5.27 has the solution

$$I_{zz} = \left[\frac{1}{12}BH^3 + 0^2(BH)\right] - \left[\frac{1}{12}bh^3 + 0^2(bh)\right] = \frac{1}{12}\left(BH^3 - bh^3\right). \tag{A5.6}$$

Hence, as in the case of composite sections and centroids (Appendix 3 of Chap. 3), we can easily add or remove the scalar second moment of areas.

Finally, it should be noted that second moments of areas, like stress and strain, obey coordinate transformation relations. Hence, if we know I_{yy}, I_{zz}, and I_{yz} in two-dimensions, then values with respect to (y', z') can be computed as (Fig. 5.28)

$$\begin{aligned} I'_{yy} &= I_{yy}\cos^2\alpha + 2I_{yz}\cos\alpha\sin\alpha + I_{zz}\sin^2\alpha, \\ I'_{zz} &= I_{yy}\sin^2\alpha - 2I_{yz}\cos\alpha\sin\alpha + I_{zz}\cos^2\alpha, \\ I'_{yz} &= \left(I_{zz} - I_{yy}\right)\cos\alpha\sin\alpha + I_{yz}(\cos^2\alpha - \sin^2\alpha), \end{aligned} \tag{A5.7}$$

although we will not prove these results here. Clearly, though, given the values of the second moments of area with respect to convenient centroidal axes,

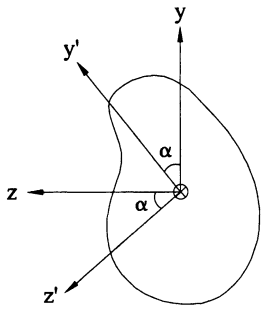

FIGURE 5.28 Similar to components of stress and strain, second moments of area relative to one coordinate system can be related easily to those of an associated coordinated system via a simple transformation.

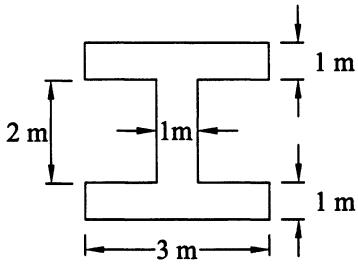

FIGURE 5.29 A dimensioned I-beam.

one can determine components for any other related coordinate system via the parallel axis theorem and/or transformation relations.

Example A5.1 Determine the second moment of area I_{zz} about the horizontal axis for the I-beam in Fig. 5.29.

Solution: For this problem, the centroid of the entire area is clear, the geometric center of the overall cross-section. To obtain I_{zz} for the whole cross section, the parallel axis theorem is used; that is,

$$I'_{zz}(\text{whole}) = \sum \left(I_{zz} + d^2 A\right)_{\text{parts}},$$

where the cross section can be broken into three parts as in Fig. 5.26 and the coordinate system located at the overall centroid. Because each part is rectangular, Eq. (A4.5) can be used to calculate $I_{zz})_c$ for each piece of the cross section. For part 1:

$$I'_{zz} = I_{zz})_c + Ad^2 = \frac{1}{12}(\text{base})(\text{height})^3 + (\text{base})(\text{height})d^2,$$

$$I'_{zz} = \frac{1}{12}(3\,\text{m})(1\,\text{m})^3 + (3\,\text{m})(1\,\text{m})(1.5\,\text{m})^2 = 7\,\text{m}^4.$$

For part 2:

$$I'_{zz} = I_{zz})_c + Ad^2 = \frac{1}{12}(\text{base})(\text{height})^3 + (\text{base})(\text{height})d^2,$$

$$I'_{zz} = \frac{1}{12}(1\,\text{m})(2\,\text{m})^3 + (1\,\text{m})(2\,\text{m})(0)^2 = \frac{2}{3}\text{m}^4.$$

For part 3:

$$I'_{zz} = I_{zz})_c + Ad^2 = \frac{1}{12}(\text{base})(\text{height})^3 + (\text{base})(\text{height})d^2,$$

$$I'_{zz} = \frac{1}{12}(3\,\text{m})(1\,\text{m})^3 + (3\,\text{m})(1\,\text{m})(-1.5\,\text{m})^2 = 7\,\text{m}^4.$$

For the composite section, therefore:

$$I'_{zz} = 7\,\text{m}^4 + \frac{2}{3}\text{m}^4 + 7\,\text{m}^4 = 14.667\,\text{m}^4.$$

Example A5.2 Determine the second moment of area I_{yy} about the horizontal x axis for an area that is shaped like a "C". Let the overall width and height be 3.5 in. and 6.0 in., respectively. Let the "cut-out" be centered vertically but toward the right and 3 in. in width and 5 in. in height.

Solution: First, sketch the cross section. Second, find the centroid of the area. To do this, visualize breaking the cross section into parts. One way to visualize the cross section is by a sum of multiple parts that are joined together. Another way to visualize it is by subtracting the hollow interior from a solid cross section. Using the second method, we must find the centroid of the entire cross section. The best way to do this is to organize a chart of the parts in order to locate the centroid relative to (x, y).

Part	Area (A)	$\bar{x}$	$\bar{y}$	$A\bar{x}$	$A\bar{y}$
1	6 in. × 3.5 in.	1.75 in	3 in	36.75 in^3	63 in^3
2	−(3 in. × 5 in.)	2 in	3 in	−30 in^3	−45 in^3
∑	6 in.^{2}			6.75 in^3	18 in^3

Thus,

$$\overline{y} = \frac{\sum A\overline{y}}{\sum A} = \frac{18\,\text{in.}^3}{6\,\text{in.}^2} = 3\,\text{in.}, \quad \overline{x} = \frac{\sum A\overline{x}}{\sum A} = \frac{6.75\,\text{in.}^3}{6\,\text{in.}^2} = 1.12\,\text{in.}$$

To calculate $I_{xx} = \iint y^2 dA$ let us use the parallel axis theorem. This is most easily done by considering a solid rectangular cross section and subtracting the hollow interior from it. Once the overall centroid has been located, originate the coordinate system there. Because each of the cross sections is rectangular, the general formula, $I_{xx})_c = (\text{l}/12)(\text{base})(\text{height})^3$, can be used. For the solid area:

$$I'_{xx} = I_{xx})_c + Ad^2 = \frac{1}{12}(\text{base})(\text{height})^3 + (\text{base})(\text{height})d^2,$$

$$I'_{xx} = \frac{1}{12}(3.5\text{ in.})(6\text{ in.})^3 + (3.5\text{ in.})(6\,\text{in.})(0)^2 = 63\,\text{in.}^4.$$

For the hollow interior:

$$I'_{xx} = I_{xx})_c + Ad^2 = \frac{1}{12}(\text{base})(\text{height})^3 + (\text{base})(\text{height})d^2,$$

$$I'_{xx} = \frac{1}{12}(3\text{ in.})(5\text{ in.})^3 + (3\text{ in.})(5\,\text{in.})(0)^2 = 31.25\,\text{in.}^4.$$

For the composite section, therefore,

$$I'_{xx} = 63\text{ in.}^4 - 31.25\text{ in.}^4 = 31.75\,\text{in.}^4$$

Now, various quantities dependent on I_{xx}, such as stress or the critical buckling load, can be calculated for this particular cross section.

Exercises

5.1. Find σ_{xx} and σ_{xy} for the following beam (Fig. 5.30). Assume a rectangular cross-section of height h and width b.

5.2. Find σ_{xx} and σ_{xy} for the following beam (Fig. 5.31), having a rectangular cross-section.

5.3. Find σ_{xx} and σ_{xy} for the following beam (Fig. 5.32), having a rectangular cross-section.

5.4. Find σ_{xx} and σ_{xy} for the following beam (Fig. 5.33), having a rectangular cross-section.

FIGURE 5.30

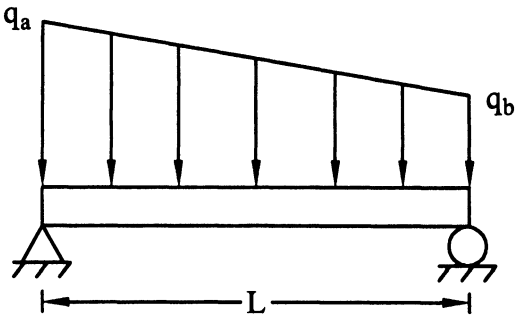

FIGURE 5.31

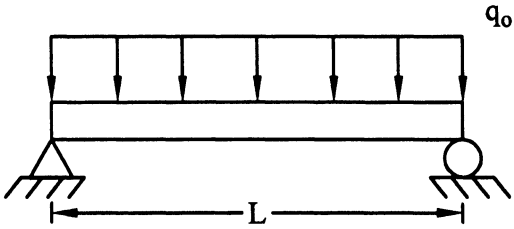

FIGURE 5.32

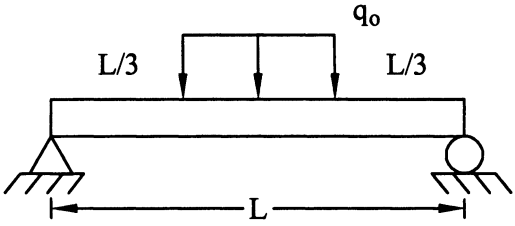

FIGURE 5.33

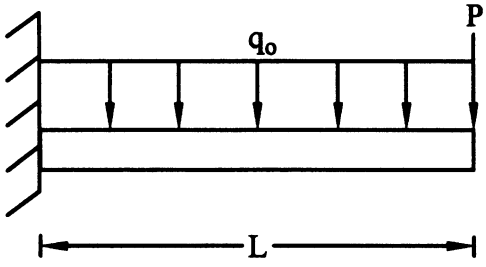

5.5. Find σ_{xx} and σ_{xy} for the following beam (Fig. 5.34), having a rectangular cross-section.

5.6. Find the maximum value of σ'_{xx} and σ'_{xy} for the beam in Exercise 5.1.

5.7. Find the maximum value of σ'_{xx} and σ'_{xy} for the beam in Exercise 5.2.

5.8. Find the maximum value of σ'_{xx} and σ'_{xy} for the beam in Exercise 5.3.

FIGURE 5.34

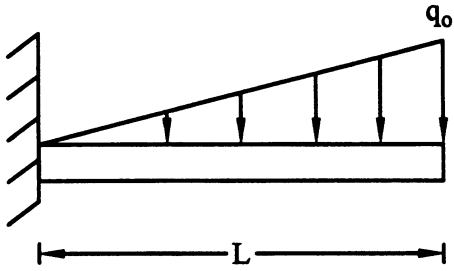

5.9. Show that $\sigma_{xy})_{\text{ave}}$ in a beam having a rectangular cross section (area $= bh$) has as its largest value $1.5\,V/A$, which is at the centroid.

5.10. Find the deflection curve for the beam in Example 5.1.

5.11. Find the deflection curve for the beam in Example 5.2.

5.12. Find the deflection curve for a simply supported beam (a pin and roller at the two ends) with a constant distributed load $q(x) = -q_o$. Note whether the beam deflects up or down.

5.13. Find the deflection curve for the beam in Exercise 5.5.

5.14. Find the deflection curve for the beam in the previous example except with a distributed load of $q(x) = (q_o/L^2)x^2$.

5.15. You are to design a force transducer based on a cantilever beam subject to an end load. Assume the beam is rectangular in cross section and that redundant strain gauges are placed at $(x = L/2, y = \pm h/2)$. Find a formula for selecting the value of Young's modulus E if the maximum allowable measured strain ε_{xx} is ε_o (i.e., find E in terms of, possibly, ε_o, L, h, b, P, etc.). Note that Popov (1999) is a nice introduction to mechanical engineering applications of strength of materials such as this problem.

5.16. Radmacher et al. (1992) pointed out that if one "drags" the AFM probe across a surface, the tip of the probe experiences both a normal force and a tangential force. The latter will contribute to the bending. Given the probe shown below, find the end deflection $\delta = v(x = L)$ (Fig. 5.35).

5.17. Using the principle of superposition, find the displacement vector $\boldsymbol{u}(x)$ of the neutral axis for the beam shown below. Hint: Let $\boldsymbol{u}(x) = v(x)\,\hat{\boldsymbol{j}} + w(x)\hat{\boldsymbol{k}}$ (Fig. 5.36).

5.18. Use the principle of superposition to find the deflection curve $v(x)$ for the neutral axis for the beam in Exercise 5.4.

5.19. Use the principle of superposition to find the reactions for a beam that is fixed on both ends and subjected to a uniformly distributed load. Hint: Assume that there is no axial load and divide the problem into three cantilever beams: one with the distributed load, one with an end load R_B, and one with an end moment M_B. Use the kinematic constraint conditions that

$$v(x = L) = 0 = v_1(x = L) + v_2(x = L) + v_3(x = L)$$

FIGURE 5.35

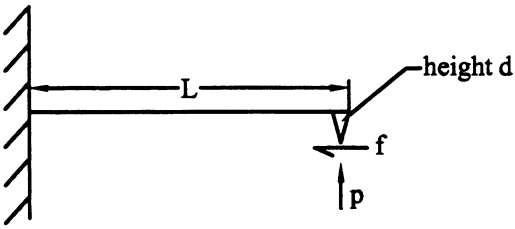

FIGURE 5.36

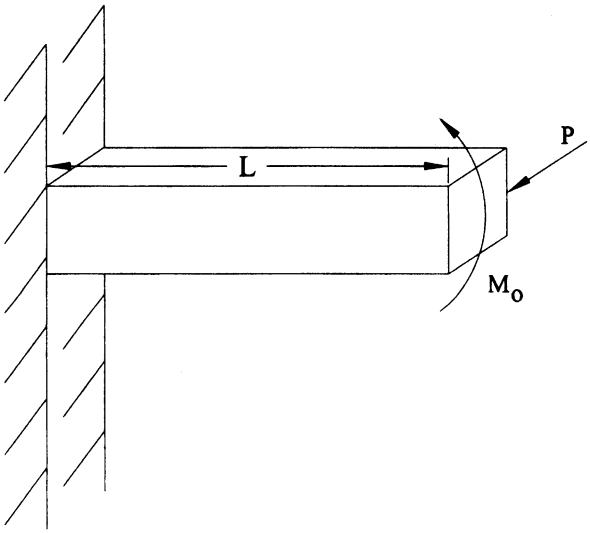

and

$$\frac{dv}{dx}(x=L)=0=\frac{dv_1}{dx}(x=L)+\frac{dv_2}{dx}(x=L)+\frac{dv_3}{dx}(x=L),$$

from which we see that we have the requisite five equations (three equilibrium and two constraints) for the five unknowns (R_x, R_A, M_A, R_B, M_B).

5.20. Two potential experiments for determining the (effective) Young's modulus E for a bone sample are the so-called three-point and four-point bending tests, shown schematically here in Fig. 5.37. Assuming that three strain gauges (A, B, C) are applied equidistantly to the bottom surface of each beam sample and that their lengths are $L/50$ each, note that the desired value of the Young's modulus can be determined via

$$\sigma_{xx}(x,y)=E\varepsilon_{xx}(x,y)\rightarrow E=-\frac{M_z(x)y}{I_{zz}\varepsilon_{xx(\text{guage})}},$$

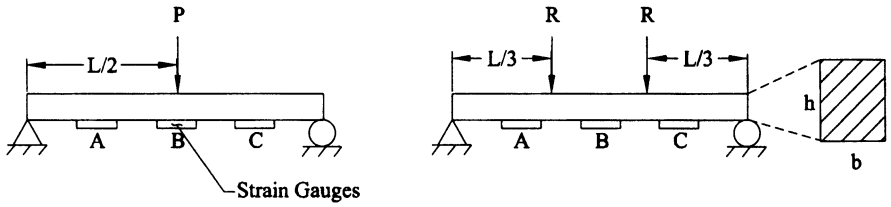

FIGURE 5.37

where x and y must correspond to the placement of one or more of the strain gauges. Via a mechanical analysis, show why the preferred measurement (of the three sites shown) would be via gauge B in the four-point bending test. Hint: Recall that a gauge is of a finite, albeit small, length, whereas strain is defined at a point.

5.21. For the three-point and four-point bending tests shown in Exercise 5.20, find the value of R in terms of P (assume given) such that the maximum value of σ_{xx} is the same in each beam. Note the value of (x, y) at which σ_{xx} is maximum.

5.22. Assume that a LEHI gate is designed as a "dam." Find the deflection curve assuming that the bottom support can be modeled as a pin and the top support as a roller (pushing opposite the force of the fluid). Hint: First determine the uniform loading on the beam gate given the differential equation for fluid statics

$$\frac{dp}{dx} = \rho g,$$

where ρ is the density of the fluid and g is the gravitational constant. Note the boundary condition that $p = p_{\text{atm}}$ at $x = 0$.

5.23. Noting that the flexure formula $\sigma_{xx} = -M_z y / I_{zz}$ was determined via an approximate, linear theory, superposition of stresses holds. Hence, for a combined axial load and bending,

$$\sigma_{xx} = \frac{f}{A} - \frac{M_z y}{I_{zz}}.$$

In like fashion, note that "symmetrical" bending due to moments applied with respect to both the z and y axes will induce a superimposed stress (Boresi et al. 1993)

$$\sigma_{xx} = \frac{M_y z}{I_{yy}} - \frac{M_z y}{I_{zz}},$$

FIGURE 5.38

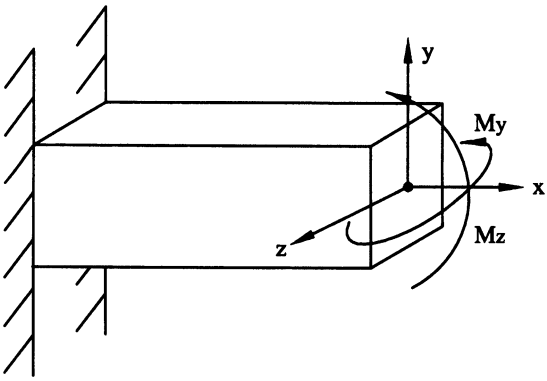

FIGURE 5.39

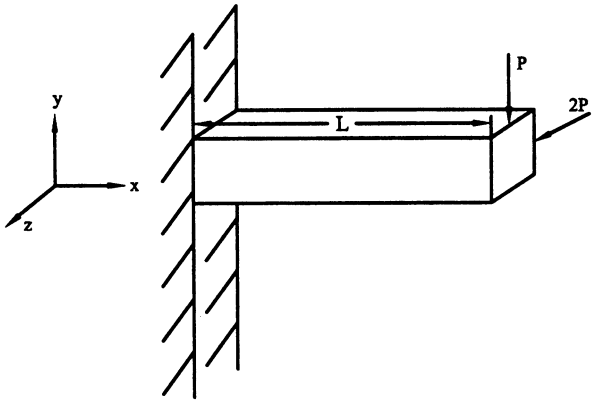

the first contribution of which can be obtained directly by deriving the flexure formula due to a moment M_y alone. Show that this is the case for the beam of length L (Fig. 5.38).

5.24. Find σ_{xy} for the beam shown in Fig. 5.39.

5.25. Whereas a moment M_z induces a bending in the x-y plane and thus a y-direction displacement, a moment M_y induces bending in the x-z plane and thus a z-direction displacement. For a combined symmetrical bending, therefore, the displacement vector $\boldsymbol{u}$ for points along the neutral axis are given by

$$\boldsymbol{u}(x) = v(x)\hat{\boldsymbol{j}} + w(x)\hat{\boldsymbol{k}}\,,$$

where

$$EI_{zz}\frac{d^2v}{dx^2} = M_z, \quad EI_{yy}\frac{d^2w}{dx^2} = M_y.$$

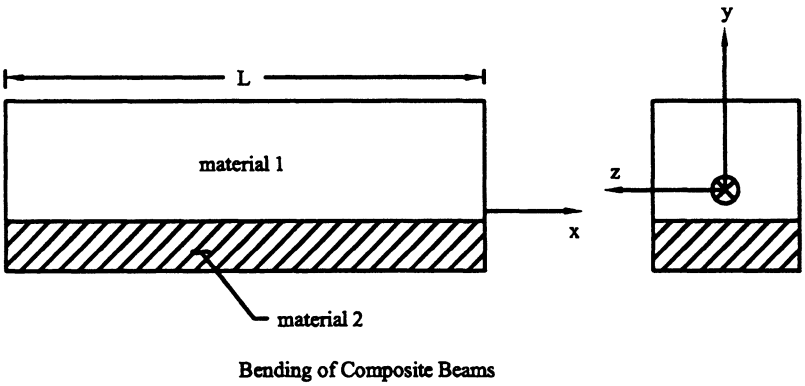

FIGURE 5.40

Hence, find $\boldsymbol{u}$ for a cantilevered beam of length L, rectangular cross section h deep and b wide and subjected to a shear force at $x = L$ given by $-P\hat{\boldsymbol{j}} + 2P\hat{\boldsymbol{k}}$ using the same figure as Exercise 5.24.

5.26. Throughout this chapter we have assumed that the cross sections are homogenous. This need not be the case. Consider the layered beam shown below (Fig. 5.40), which consists of two materials characterized by LEHI properties $E^{(1)}$, $\nu^{(1)}$ and $E^{(2)}$, $\nu^{(2)}$, respectively (note: these are Young's moduli and Poisson's ratios). If we assume a continuous strain, then $\varepsilon_{xx} = -y/\rho$ as earlier, where ρ is the radius of curvature of the neutral axis, which need not be at the centroid as in the case of a homogenous beam. Indeed, the neutral axis can be found from the axial force balance equation

$$\sum F_x = 0 = -\iint \sigma_{xx} dA = -\left[\iint \sigma_{xx}^{(1)} dA^{(1)} + \sigma_{xx}^{(2)} dA^{(2)}\right],$$

where

$$\sigma_{xx}^{(1)} = E^{(1)}\varepsilon_{xx}, \quad \sigma_{xx}^{(2)} = E^{(2)}\varepsilon_{xx}.$$

Hence, the neutral axis is located by

$$E^{(1)}\iint y dA^{(1)} + E^{(2)}\iint y dA^{(2)} = 0,$$

wherein the $-1/\rho$ was factored out. Show that this recovers the result for a homogeneous beam if $E^{(1)} = E^{(2)}$ and if $A^{(1)} + A^{(2)} = A$, the total cross-sectional area. Note, too, that from moment balance, we get

$$-M_z + \iint -\sigma_{xx}\, y\, dA = 0$$

$$\rightarrow M_z = -\iint -\frac{E^{(1)}}{\rho} y^2\, dA^{(1)} - \iint -\frac{E^{(2)}}{\rho} y^2\, dA^{(2)}.$$

Show that this leads to the following moment-curvature relation:

$$\frac{1}{\rho} = \frac{M_z y}{E^{(1)} I_{zz}^{(1)} + E^{(2)} I_{zz}^{(2)}}$$

and thus

$$\sigma_{xx}^{(1)} = -\frac{M_z y E^{(1)}}{E^{(1)} I_{zz}^{(1)} + E^{(2)} I_{zz}^{(2)}}, \quad \sigma_{xx}^{(2)} = -\frac{M_z y E^{(2)}}{E^{(1)} I_{zz}^{(1)} + E^{(2)} I_{zz}^{(2)}},$$

where

$$I_{zz}^{(1)} + I_{zz}^{(2)} = I_{zz}.$$

5.27. Locate the neutral axis for the composite cross section (Fig. 5.41). Hint: Assume that the neutral axis (i.e., origin of y-z axes) is at the centroid, but then find its true value relative to the interface between materials 1 and 2. Toward this end, note that

$$\iint y\, dA^{(1)} = \int_{-b/2}^{b/2} \int_{-H}^{h^{(1)}-H} y\, dy\, dz = \frac{b}{2}\left[\left(h^{(1)}\right)^2 - 2Hh^{(1)}\right],$$

$$\iint y\, dA^{(2)} = \int_{-b/2}^{b/2} \int_{-\left(h^{(2)}-H\right)}^{-H} y\, dy\, dz = -\frac{b}{2}\left[\left(h^{(2)}\right)^2 - 2Hh^{(2)}\right],$$

FIGURE 5.41

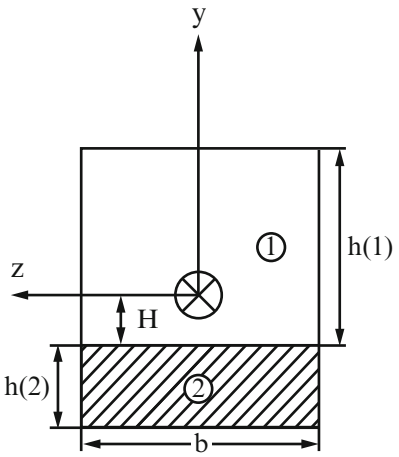

where H is the distance (assumed down) from the centroid to the interface between material 1 and material 2. Thus, axial force balance yields

$$H = \frac{1}{2}\left(\frac{E^{(1)}\left(h^{(1)}\right)^2 - E^{(2)}\left(h^{(2)}\right)^2}{E^{(1)}h^{(1)} + E^{(2)}h^{(2)}}\right).$$

Note that if $E^{(1)} = E$, $E^{(2)} = 0$, $h^{(1)} = h$, and $h^{(2)} = 0$, then $H = h/2$, thus locating the neutral axis at the centroid, as it should for a homogenous beam.

5.28. In cardiopulmonary resuscitation (CPR), one seeks to augment cardiac output by pressing down on the sternum. This increases blood flow by direct compression of the heart between the sternum and spine as well as via changes in intrathoracic pressure. Typically, the sternum is compressed 1.5–2 in. with each compression. One concern in CPR, however, is that excessive force may fracture the ribs. Referring to Fig. 5.42, we see that the transversely applied load P induces bending stresses in the rib. If you are biomedical engineer charged with designing an automatic device to load the sternum, find the induced stresses in the ribs as a function of the applied load and geometry. Hint: The rib can be assumed to exhibit a LEHI behavior and it is a structure having one dimension much larger than the other two and subjected to bending. The ribs are clearly not initially straight beams, thus our flexure formula does not apply. It can be shown, however, that the bending stress in a curved beam can be computed via (Boresi et al. 1993)

$$\sigma_{\theta\theta} = \frac{f}{A} + \frac{M(A - rA_m)}{Ar(RA_m - A)},$$

where f is a force applied normal to the θ-face cross section of area A, M is the bending moment, $A_m = \int (1/r)dA$, where r is the radial location of the point of interest in the cross section, and R is the radial distance from the center of curvature of the beam to the centroid of the cross section (see figure). Because we have merely listed, not derived, this formula, we must note the assumptions/restrictions. First, plane sections are assumed to remain plane; the radial stress σ_{rr} and shear stress $\sigma_{\theta r}$ are assumed to be small in comparison to $\sigma_{\theta\theta}$, the cross section is assumed to be symmetric about the vertical y axis shown in the figure; the applied loads all lie in the plane of symmetry; and $R/h < 5$. In other words, if $R/h > 5$, the flexure formula [Eq. (5.23)] is often used even for a curved beam. Finally, see Table 5.1 for formulas for A and A_m for common cross sections.

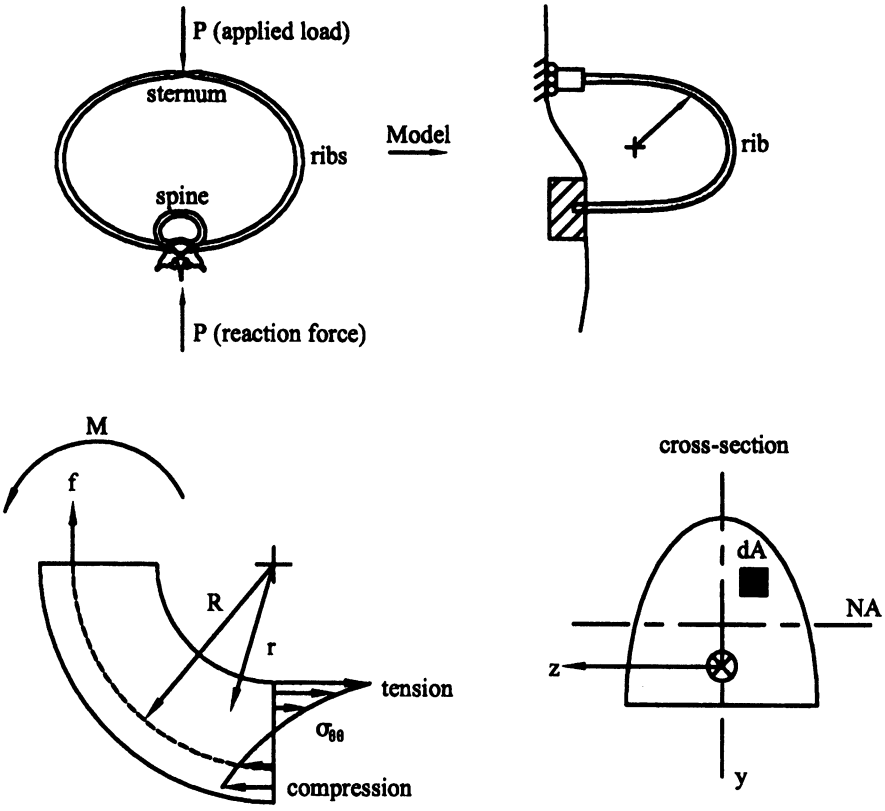

FIGURE 5.42

5.29. Show that the critical load for a fixed–fixed column subjected to an end load P is

$$P_{cr} = \frac{4\pi^2 EI_{zz}}{L^2}.$$

5.30. Show that the critical load for a pinned–pinned column subjected to an end load P is

$$P_{\text{cr}} = \frac{\pi^2 EI_{zz}}{L^2}.$$

TABLE 5.1 Formulae for A and A_m for curved beams having different cross-sections. Note the coordinate directions. See Boresi et al. (1993).

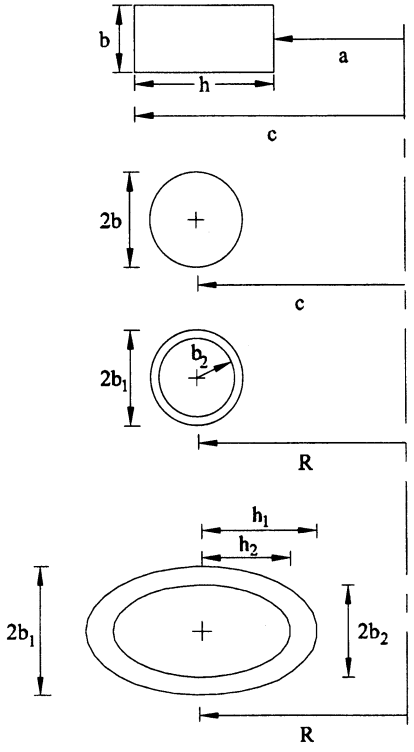

$$A = b(c-a)$$
$$A_m = b\ln(c/a)$$
$$R = \frac{a+c}{2}$$

$$A = \pi b^2$$
$$A_m = 2\pi(R - \sqrt{R^2 - b^2})$$

$$A = \pi(b_1^2 - b_2^2)$$
$$A_m = 2\pi(R^2 - b_2^2 - R^2 - b_1^2)$$

$$A = \pi(b_1 h_1 - b_2 h_2)$$
$$A_m = 2\pi\left(\frac{b_1 R}{h_1} - \frac{b_2 R}{h_2} - \frac{b_1\sqrt{R^2 - h_1^2}}{h_1} + \frac{b_2\sqrt{R^2 - h_2^2}}{h_2}\right)$$